Amino Acids (2011) 41:235–256
DOI 10.1007/s00726-010-0682-4

REVIEW ARTICLE

Modern developments in mass spectrometry of chondroitin and dermatan sulfate glycosaminoglycans

Eugen Sisu · Corina Flangea · Alina Serb · Alina D. Zamfir

Received: 3 March 2010 / Accepted: 29 June 2010 / Published online: 15 July 2010

Abstract Chondroitin sulfate (CS) and dermatan sulfate (DS) are special types of glycosaminoglycan (GAG) oligosaccharides able to regulate vital biological functions that depend on precise motifs of their constituent hexose sequences and the extent and location of their sulfation. As a result, the need for better understanding of CS/DS biological role called for the elaboration and application of straightforward strategies for their composition and structure elucidation. Due to its high sensitivity, reproducibility, and the possibility to rapidly generate data on fine CS/DS structure determinants, mass spectrometry (MS) based on either electrospray ionization (ESI) or matrix-assisted laser desorption/ionization (MALDI) brought a major progress in the field. Here, modern developments in MS of CS/DS GAGs are gathered in a critical review covering the past 5 years. The first section is dedicated to protocols for CS/DS extraction from parent proteoglycan, digestion, and purification that are among critical prerequisites of a successful MS experiment. The second part highlights several MALDI MS aspects, the requirements, and applications of this ionization method to CS/DS investigation. An ample chapter is devoted to ESI MS strategies, which employ either capillary- or advanced chip-based sample infusion in combination with multistage MS (MS^n) using either collision-induced (CID) or electron detachment dissociation (EDD). At last, the potential of two versatile separation techniques, capillary electrophoresis (CE), and liquid chromatography (LC) in off- and/or on-line coupling with ESI MS and MS^n, is discussed, alongside an assessment of particular buffer/solvent conditions and instrumental parameters required for CS/DS mixture separation followed by on-line mass analysis of individual components.

Keywords Chondroitin/dermatan sulfate · Mass spectrometry · MALDI · ESI · Chip-nanoESI · Capillary electrophoresis · HPLC · Screening · Sequencing · Review

E. Sisu · A. Serb
Department of Biochemistry, "Victor Babes" University of Medicine and Pharmacy, 300054 Timisoara, Romania

E. Sisu
Chemistry Institute of Romanian Academy, 300223 Timisoara, Romania

C. Flangea · A. D. Zamfir
Department of Chemical and Biological Sciences, "Aurel Vlaicu" University of Arad, 310130 Arad, Romania

A. D. Zamfir (✉)
Mass Spectrometry Laboratory, National Institute for Research and Development in Electrochemistry and Condensed Matter, Plautius Andronescu Str. 1, 300224 Timisoara, Romania
e-mail: alina.zamfir@uav.ro

Introduction

Proteoglycans (PGs) are an important class of biomacromolecules, which show the largest and most complex molecular structures of world life. PGs are major components in the extracellular matrix, basement membranes being present also in the intracellular region. They are composed of a core protein and glycosaminoglycans (GAGs) chains. Many other oligosaccharide chains are attached either as *O*-glycosides with the hydroxyl groups of the side chains of serine, threonine, or other hydroxyl amino acid residues or as *N*-glycosyl groups through linkage to the amide groups of asparagine side chains. Both types of linkages may be present in a single protein (Fig. 1).

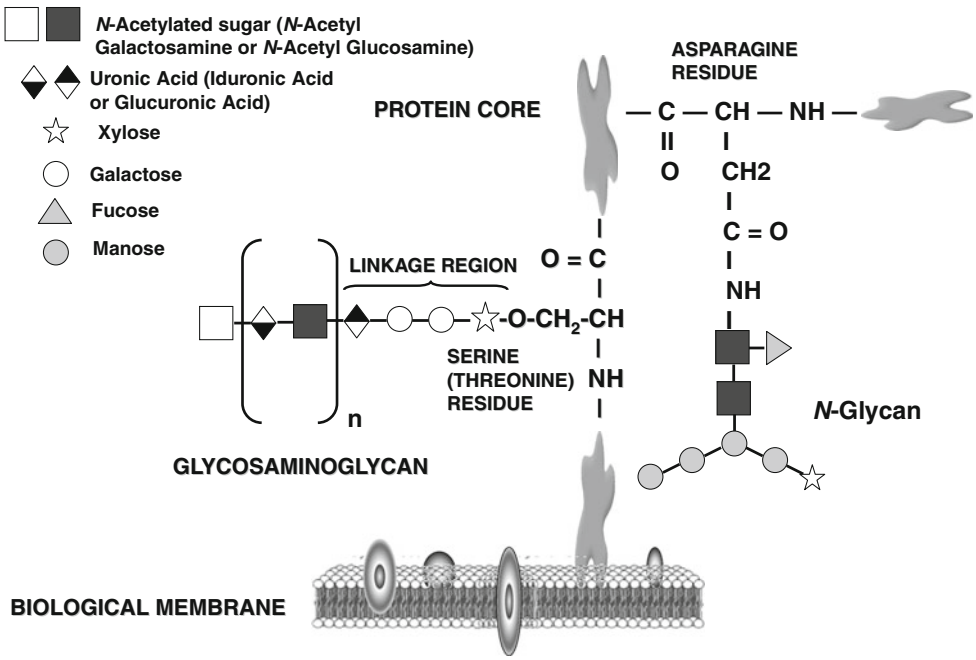

Fig. 1 Schematic of proteoglycan structure

Glycosaminoglycans (GAGs) can be divided into two subgroups: (a) the glucosaminoglycans encompassing hyaluronic acid (HA), keratan sulfate (KS), heparan sulfate (HS), and heparin and (b) galactosaminoglycans, which include chondroitin and dermatan sulfate (CS/DS). Each GAG is a polymer of repeating disaccharides encompassing a hexosamine and a non-nitrogenous sugar, which is usually an uronic acid, except for KS, in which this hexose is D-galactose. Except for KS and HA, all GAGs are linked to their parent protein via xylose–galactose–galactose–glucuronic acid core tetrasaccharide (GlcAβ1-3Galβ1-3Galβ1-4Xylβ1-*O*-Ser).

Hyaluronic acid (HA) is a high molecular weight (105–107 kDa) linear GAG consisting of β(1-3)-*N*-acetyl-D-glucosamine β(1-4)-D-glucuronic acid repeats. Unlike other GAGs, HA is found in nature as a free chain, which is neither differentially sulfated nor epimerized (Toole 2004; Seyfried et al. 2005).

Keratan sulfate (KS) is a GAG formed through the elongation of *N*- or *O*-glycans covalently attached to scaffold proteins. KS is composed of repeating disaccharide units of galactose and *N*-acetylglucosamine (GlcNAc) linked β(1-4) and β(1-3), with sulfate groups at the C6 positions of galactose and GlcNAc. The sulfation modification of GlcNAc residues is mediated by GlcNAc-6-*O*-sulfotransferase, which is critical for KS synthesis. KS is also expressed in central nervous tissues where its synthesis is up-regulated in the lesions on central nervous system (CNS) injury (Zhang et al. 2005, 2006).

Heparin and HS are polydisperse linear polymers that share structural similarities. They are composed of alternate units of α-D-glucosamine (GlcN) and uronic acid, either β-D-glucuronic acid (GlcA) or α-L-iduronic acid (IdoA), joined together by (1-4) glycosidic linkages. In HS, GlcN can be either *N*-sulfated or *N*-acetylated, whereas in heparin the *N*-acetyl groups correspond to less than 5%. 2-*O*-sulfated iduronic acid–*N*,6-disulfated glucosamine are major components of the *N*-sulfated (NS) region, which is prevalent (>70%) in heparin, while glucuronic acid–*N*-acetylated glucosamine is a component of the less abundant *N*-acetylated (NA) and mixed (NA/NS) regions, respectively. One of the most important features of heparin/HS is their ability to interact with a wide array of proteins. Heparin/HS also exert a regulatory role by modulating the activity of the proteins with which they interact (Naimy et al. 2008).

Chondroitin and dermatan sulfate (CS/DS) consists of repeating disaccharide units of HexA β(1-3) GalNAc β(1-4) that are polymerized in chains of size varying from 20 to 50 kDa depending on the core protein, tissue location, and disease contexts. The chain is a mixture of domains with high or low IdoA/GlcA content of differing sulfation patterns (Hitchcock et al. 2006). Many types of CS exist, however, the three main classifications of CS found in higher animals include CS type A (CS A), CS type B (CS B, otherwise known as DS, or dermatan sulfate), and CS type C (CS C). CS A is most commonly sulfated (90%) at the C4-position of GalNAc, while CS C is most commonly sulfated (90%) at the C6-position of GalNAc. CS B contains a high percentage of repeats in which GlcA is epimerized to IdoA. A fraction of such repeats are sulfated at the C2-position of iduronic acid. CS B is most often sulfated at the C4-position of GalNAc. Other rare CS/DS glycoforms (Fig. 2) are CS D (GlcA2S-GalNAc6S), CS E

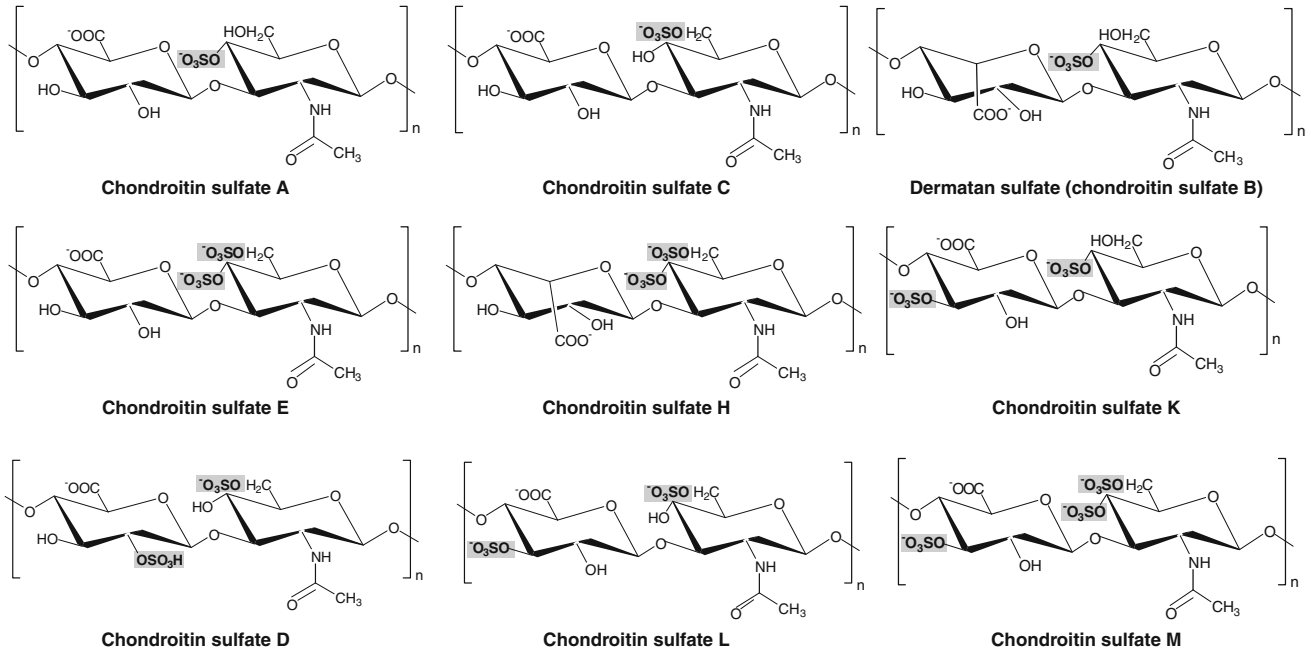

Fig. 2 Detailed structures of repeating disaccharide units in various CS types

(GlcA-GalNAc4,6S), CS K (GlcA3S-GalNAc4S), CS L (GlcA3S-GalNAc6S), and CS M (GlcA3S-GalNAc4S,6S).

Previous reports suggested that isomeric CS glycoforms differing in position and degree of sulfation play specific and distinct functional roles during development (Tufvesson and Malmstrom 2002). The disulfated CS D (~20%) and CS E (~60%) disaccharide units are characteristic components in shark cartilage and squid cartilage, respectively, but are also found in mammalian DS chains (Sugahara and Yamada 2000). The oversulfated CS H, isolated from the hagfish notochord, contains a high proportion (68%) of the disaccharide H (or iE) unit (IdoA-GalNAc4S,6S), which is also found in other DS chains (Sugahara and Yamada 2000). 3-*O*-sulfation of GlcA is a non-common structural modification, leading to some rare disaccharide units, such as the K, L, M identified in polysaccharides from marine invertebrates.

Recent studies have shown that proportions of CS/DS disaccharides in brain change with development/affliction, which suggests that CS/DS species differing in the degree and profile of sulfation are correlated with the functional diversity of neurons (Purushothaman et al. 2007). Oversulfated CS, DS, and hybrid CS/DS structures have been found strongly implicated in brain development (Bao et al. 2005).

CS/DS is attached to different core proteins, such as biglycan, decorin, versican, aggrecan, perlecan, and syndecan. Decorin and biglycan are members of the small leucine-rich family of PGs that are substituted with one or two CS/DS GAG chains, while versican and aggrecan belong to the hyalectin family. Hyalectins are a group of large PGs that can form aggregates with HA. They also form large complexes with fibrous matrix proteins, such as collagen. Evidence shows that they can affect the activity and stability of proteins and signaling molecules within the extracellular matrix (Schwartz and Domowicz 2004).

In the last decade mass spectrometry (MS) based on either electrospray ionization (ESI) or matrix-assisted laser desorption/ionization (MALDI) alone or in conjunction with hyphenated techniques, such as capillary electrophoresis (CE) and high performance liquid chromatography (HPLC) developed as the most efficient analytical tool for GAG analysis in general and CS/DS in particular. A high number of valuable review articles (Zaia 2004, 2009; Seidler et al. 2007; Amon et al. 2008, Volpi et al. 2008) emphasized in recent years the major contribution of ESI and MALDI MS in compositional and structural elucidation of various GAG structures. However, MS-based analysis of CS/DS was not the exclusive focus of a thorough review article so far. To close this gap we present here an overview on this topic, covering the last 5 years. The purpose of our survey is to update the reader with the most recent contributions in the field and to complement the review literature existing so far.

Procedures of CS/DS extraction and preparation for MS

Isolation and purification of CSPG

To extract CSPGs in intact form, inhibition of core protein degradation is essential. Therefore, tissues should be

excised on ice and should be quickly frozen and kept in a deep freezer or in liquid nitrogen. However, in the case of extraction of CSPGs associated with membranes, usually membrane fractions are prepared from the freshly excised tissues because freezing and thawing disrupt cell membranes. In some cases, tissue-specific pretreatments are made before extraction of PGs. For example, mineralized tissues, such as bones and teeth need to be frozen and grinded (Fedarko 2001) prior to the application of PG extraction procedures. For extraction of brain PGs, the fresh brain tissue is subjected to grinding followed by overnight immersion in a 4 M guanidium chloride solution (Flangea et al. 2009b) at 4°C, while gently stirred. The incubation in guanidium chloride is necessary for denaturation of brain tissue proteins. Following this step the solution containing brain tissue is centrifuged for few minutes and the resulting supernatant is collected for PG extraction. PGs are extracted from tissues with a saline solution usually containing denaturing agents and/or detergents; then they are separated from other proteins by a combination of separation methods including ultracentrifugation, ion-exchange chromatography, and gel chromatography. Antibodies are also useful tools to purify the corresponding PGs. Many antibodies are now available for particular domains of CS and core proteins of individual CSPGs. An exhaustive protocol related to the isolation and purification of CSPG is already available (Matsui and Oohira 2006).

Isolation and purification of CS/DS

To obtain free CS/DS chains, β-elimination is carried out usually in 0.15 M NaOH and 1 M $NaBH_4$ for 24 h at 37°C followed by neutralization with acetic acid and applied on diethylaminoethyl (DEAE)-tris(hydroxymethyl)aminomethane (Tris)-Acryl-M anion-exchange column. Several procedures can be used to isolate CS/DS from other GAG species present in a mixture after tissue extraction, such as sequential precipitation with organic solvents, fractionation by using anion-exchange chromatography, and degradation of single species of GAGs by highly specific enzymes followed by gel-permeation chromatography (Hernáiz and Linhardt 2001). Fractional precipitation with ethanol is one of the classical methods for the separation of GAG mixtures. In favorable situations, the method can be applied directly to a tissue digest (Hernáiz and Linhardt 2001).

Obtained purified CS/DS chains are enzymatically digested with different types of chondroitin lyases (EC 4.2.2.-). Among chondroitin lyases, those acting specifically on CS/DS chain have been biochemically classified as chondroitinases ABC, AC, B, and C depending on their substrate specificities (Hernáiz and Linhardt 2001). Because of the specificity of the lyase, the origin of the Δ-HexA in the oligosaccharides is known.

Chondroitinase ABC from *Pedobacter heparinus* (*Flavobacterium heparinum*) is a lyase that exhibits broad substrate specificity, acting on a variety of GAGs, including C4S, C6S, DS, chondroitin, and chondroitin D and E. The enzyme is unable to catalyze the depolymerization of hyaluronate, heparin and HS, or KS but is fully active against DS. Chondroitinase ABC from *Proteus vulgaris* comprises two distinct lyases: ABC I and ABC II. Chondroitinase ABC I optimally processes CS and DS substrates. The products of an exhaustive digestion of CS or DS comprise a mixture of unsaturated tetrasaccharides and disaccharides (Prabhakar et al. 2005). Chondroitinase ABC II is just as broad as chondroitin ABC I in terms of substrate profile, but it is a far less efficient enzyme regarding catalytic activity (Hamai et al. 1997).

Chondroitinase AC from *Pedobacter heparinus* (*Flavobacterium heparinum*) acts on C4S, C6S, chondroitin, and hyaluronate (Huang et al. 2001) being completely incapable of DS cleavage. Heparin and DS are notable inhibitors of enzyme activity (Pojasek et al. 2001; Rye and Withers 2002). Chondroitinase AC from *Arthrobacter aurescens* (Lunin et al. 2004) acts on C4S, C6S, chondroitin, and hyaluronan and is also inhibited by DS. The enzyme processes these substrates exolytically, generating almost exclusively disaccharide products. Chondroitinase AC cleaves CS/DS copolymers, but only at linkages containing GlcA (Zhang et al. 2009).

Chondroitinase B from *Pedobacter heparinus* (*Flavobacterium heparinum*) (Michel et al. 2004) is the only known lyase that cleaves DS as its sole substrate. Chondroitinase B may cleave DS β(1,4) bonds that contain the commonly occurring 4-*O*-sulfate, but also linkages with sulfation at the 2-*O* and 6-*O*-positions, or both.

After depolymerization with chondroitin lyases, the CS/DS oligosaccharide mixture is applied on size exclusion chromatography, and the collected fractions are submitted for MS experiments usually dissolved in 20 mM ammonium acetate in deionized water/MeOH (Seidler et al. 2007) for determination of sulfate content and position.

Mass spectrometry approaches for CS/DS analysis

MALDI MS

MALDI MS may be efficiently applied not only for the analysis of chromatographic fractions containing GAG oligosaccharides in an off-line mode, but also for complex mixture investigations (Laremore et al. 2007; Zaia 2009). Its ability to create mostly singly charged species, as opposed to the multiply charged ions produced by ESI MS, greatly simplifies the interpretation of the data. Other advantages of MALDI MS over ESI MS methodologies

are: (a) applicability to high-throughput experiments; (b) robustness; (c) a relatively high tolerance to salts and other contaminants (Tissot et al. 2008). However, under conventional MALDI conditions, polyanionic oligosaccharides, such as CS/DS exhibit poor ionization efficiencies (Zaia 2004) and have the tendency to fragment through the loss of SO_3 (Laremore et al. 2007). Nevertheless, because of their propensity to form adducts with cations, sulfated oligosaccharides can be analyzed by positive ion mode MALDI MS in a form of noncovalent complexes with basic peptides, such as $(Gly–Arg)_n$, where n exceeds the number of sulfate groups by one (Deepa et al. 2007). While this method is sensitive and produces MALDI mass spectra in which SO_3 loss is suppressed, it is limited by the availability of synthetic peptides.

In addition to using the peptide complexation method to prevent GAG oligosaccharide fragmentation, double-permethylation improves the characterization of sulfated glycans by positive ion mode MALDI MS (Lei et al. 2009). Samples are first permethylated, leaving the sulfate group intact (Taguchi et al. 1996; Khoo et al. 1983). This permethylation step also stabilizes sialylated structures during methanolysis (Cointe et al. 1998) and the MS process (Kim et al. 2006). The sulfate group is then cleaved by mild acidic methanolysis, while the hydroxyl groups formed as a result of this cleavage are either permethylated or deuteromethylated. As a result of this treatment, the sulfate group is substituted by a deuteromethyl group, which is stable during MALDI MS analysis. This permethylation step also enhances MS ionization and fragmentation (Kang et al. 2005, 2008). The number of sulfate groups is easily deduced by calculating the mass shift between the spectra of permethylated and doubly permethylated analytes. The position of sulfate groups, on the other hand, can be determined by comparing the collision-induced dissociation (CID) spectra of permethylated–desulfated–permethylated (PP) and permethylated–desulfated–deuteromethylated (PD) samples (Lei et al. 2009).

The intact GAG polysaccharides cannot be detected by MS methods due to their extremely low volatilities: difficulties to evaporate saccharides increase significantly with their molecular weights and the presence of charged functional groups (sulfate residues). However, this problem can be overcome because all natural GAGs can be easily fragmented into defined oligosaccharides by enzymatic digestion (Nimptsch et al. 2009).

Regarding the type of matrices used for MALDI ionization process, 2,5-dihydroxybenzoic acid (DHB), one of the early matrices to be used for carbohydrate investigation is still the most widely employed for GAG structural analysis by MALDI MS (Nimptsch et al. 2009; Matsuno et al. 2007; Sugiura et al. 2007; Deepa et al. 2007). Ionic liquid matrices (ILMs) have a number of advantages over conventional crystalline matrices including the homogeneity of the analyte-matrix mixture, high vacuum stability of the matrix and increased shot-to-shot reproducibility (Tholey and Heinzle 2006). The possibility to perform experiments with ILMs at room temperature for the analysis of uncomplexed polysulfated oligosaccharides has been explored recently (Laremore et al. 2006, 2007). By using 1-methylimidazolium R-cyano-4-hydroxycinnamate (ImCHCA) and butylammonium 2,5-dihydroxybenzoate (DHBB) as matrices it was possible to achieve ionization of uncomplexed, underivatized, polysulfated oligosaccharides under UV-MALDI conditions, but, to some extent, both analytes have undergone thermal fragmentation, which led to the loss of SO_3 (Laremore et al. 2006, 2007).

Recent reports (Ohara et al. 2009; Laremore et al. 2007) showed that the use of a new ILM, bis-1,1,3,3-tetramethylguanidinium R-cyano-4-hydroxycinnamate (G2CHCA), facilitates positive ion mode MALDI TOF MS analysis of CS/DS at reasonable sensitivities. Purified single components of polysulfated DS oligosaccharides up to decasaccharide as well as mixtures of DS and CS oligosaccharides obtained by CS and DS depolymerization using chondroitin ABC lyase could be successfully analyzed using G2CHCA due to matrix high tolerance to buffer salts as well as the suppression of SO_3 loss (Laremore et al. 2006). In addition, CS A disaccharides resulted from enzymatic depolymerization of bovine tracheal CS A with chondroitin ABC lyase were analyzed as sodium and cesium salts using the above-mentioned ILM for MALDI TOF MS analysis (Laremore and Linhardt 2007). Conversion of CS A sodium salts into the cesium salts shifted their MALDI MS peaks toward higher m/z values (Fig. 3), which permitted the use of matrix suppression settings of up to 500 Da without inhibiting the analyte signal. A significant improvement in the MALDI MS signal of the cesium salt of CS A disaccharide as compared to that of the sodium salt of CS A disaccharide resulted from the increased stability of sulfate half-esters toward thermal fragmentation. The complete absence of SO_3 loss in the positive ion MALDI mass spectra acquired for the sodium and cesium salts of CS A disaccharide makes this method potentially applicable to the analysis of GAG-derived disaccharide mixtures having various levels of sulfation (Laremore and Linhardt 2007).

In another report (Matsuno et al. 2007), hexasaccharides at the GAG–protein linkage region from some CSPG, such as urinary trypsin inhibitor, bovine nasal cartilage proteoglycan, bovine aggrecan, bovine decorin, and bovine biglycan, were released from the protein core using the AutoGlycoCutter (AGC). AGC is an automated bench top apparatus for releasing *O*-linked-type oligosaccharides on the basis of an in-line flow system (Matsuno et al. 2007). Released oligosaccharides were labeled with 2-aminobenzoic acid (2AA)

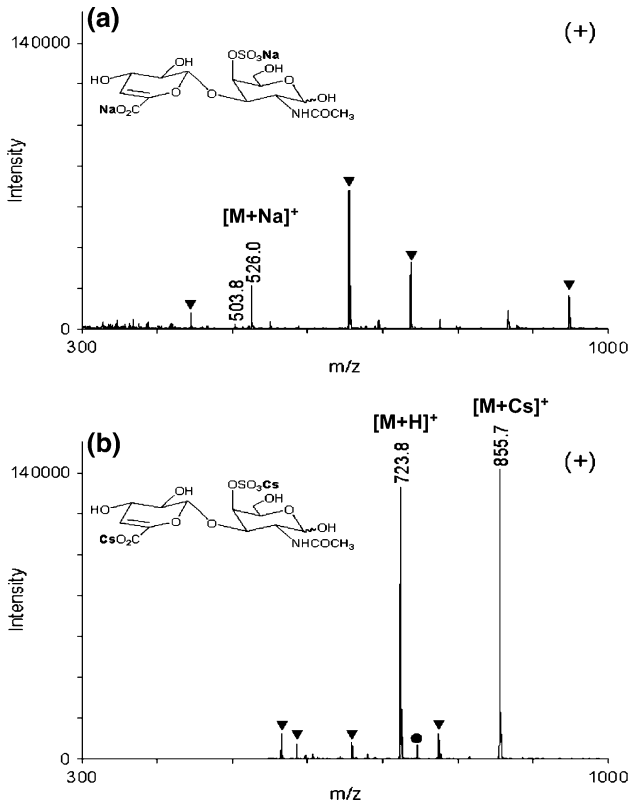

Fig. 3 Positive ion MALDI mass spectra of CS A disaccharide, sodium salt (**a**) and cesium salt (**b**) acquired with G2CHCA as a matrix. Peaks due to the matrix are marked with *triangles*. Peak marked with *closed circle* in **b** corresponds to a product of Cs/Na exchange. Reprinted and adapted with permission from (Laremore and Linhardt 2007)

and analyzed by CE and linear MALDI TOF MS in negative ion mode. DHB used as a matrix allowed to obtain the molecular ions corresponding to monosulfated and non-sulfated hexasaccharide at *m/z* 1210.9 and 1130.9, respectively (Matsuno et al. 2007).

Recently Ohara's group (Ohara et al. 2009) developed a protocol that could determine in a single experiment the degrees of polymerization and sulfation of the polysulfated-derived oligosaccharides. The method is based on negative and positive ionization modes MALDI MS using pyrenemethylguanidine (PMG) to establish noncovalent sulfate–guanidinium interactions. Unique PMG-complex ladders of peaks have been observed for all of the CS from di- to decasaccharides. Without PMG no signal could be observed; however, the addition of PMG gave a ladder of peaks dependent on the number of sulfate groups in both ionization modes. An illustrative example is presented in Fig. 4 for a tetrasulfated CS D tetrasaccharide. Mass spectra of all analyzed CS, followed the general formula of n peaks in the negative mode and $[n + 1]$ peaks in the positive mode, where n is the degree of sulfation of the analytes. In the positive ionization mode these results indicate that all SO_3 groups are bound to a PMG molecule as is one of the carboxylate groups. This result seems to indicate that the sulfate–PMG complex is stronger than the carboxylate–PMG one. In contrast, the negative ion analysis indicates that one of the sulfate groups is always staying free (Ohara et al. 2009).

MALDI TOF MS was also employed to characterize the chondroitin polymerization reaction using K4CP chondroitin polymerase from *Escherichia coli* in the presence of Mn^{2+} ions. MALDI TOF MS gave individual and continuous peaks of different chain lengths with accurately determined molecular weight. Moreover, these experiments confirmed the alternate addition of GalNAc and GlcA residues to the non-reducing end of the chondroitin hexasaccharides initial acceptor for both short-time (30 min and 1 h) (Fig. 5) and long-time (18 h) reactions (Fig. 6) (Sugiura et al. 2007). MALDI TOF MS was able to provide detailed structural information on the chains that cannot be obtained by other analytical systems. The method also enabled the identification of a large group of chondroitin oligo/polysaccharide, the largest polysaccharide ion peak being an 88-mer (bis-sodium salt, *m/z* 16.752) (Sugiura et al. 2007).

A few years ago, a complete MALDI MS analysis of the composition of CS E from squid cartilage (Deepa et al. 2007) was reported. After total digestion of squid cartilage CS E with hyaluronidase, the complex mixtures of octa- and decasaccharides were separated into 23 subfractions by anion-exchange HPLC. Delayed extraction (DE) MALDI TOF MS was used to assign the sugar and sulfate composition of the octa- and decasaccharides. As much as 11 octasaccharides and 6 decasaccharides were identified of which 8 octa- and 6 decasaccharides were previously unknown. This method was the first MALDI report in which sequencing of CS chains longer than octamer was achieved (Deepa et al. 2007).

Although different methods of CS determination do already exist (Otsuki et al. 2008; Volpi 2007; Zinellu et al. 2007), quantitative determination of CS by MALDI MS was only recently implemented (Nimptsch et al. 2009). A convenient and sensitive protocol to determine the amount of CS disaccharides in biological samples by using the easily available values of signal-to-noise (S/N) ratio was recently achieved using negative ion MALDI TOF MS (Nimptsch et al. 2009). Although, the authors expected a linear relationship between the S/N ratio and the amount of CS on the sample plate at least in a certain concentration range, the corresponding S/N ratio could be accurately fitted with a sigmoidal curve. Even though it is pointed out that there is a limited concentration range (5–30 pmol) where the S/N ratio correlates directly with the amount of CS on the sample plate. Detection limits in the picomole range clearly indicate the sensitivity of the developed

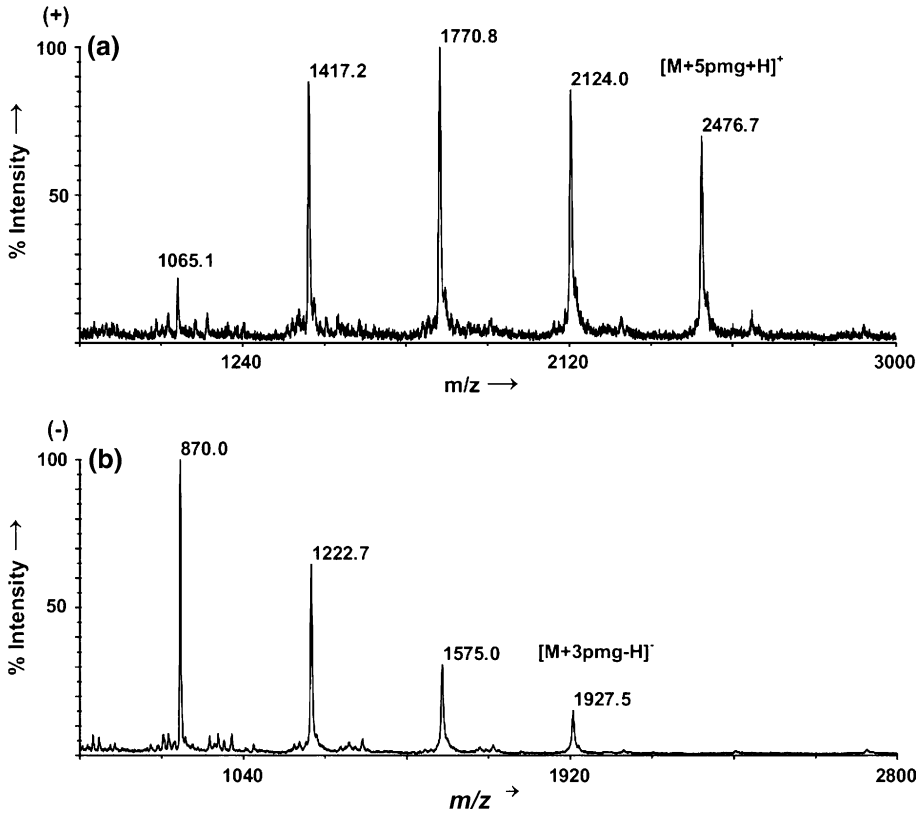

Fig. 4 Positive (**a**) and negative ion (**b**) MALDI mass spectra of CS D tetrasaccharide with PMG. In the positive mode, the five peaks obtained correspond to the complexation of 5 PMG with the oligosaccharide. The fully complexed ion is easily detected at *m/z* 2,476.7. In the negative mode, four well-distinguished peaks can be observed, with the highest *m/z* value at 1,927.5 corresponding to a complexation of CS D tetra with 3 PMG molecules. The mass differences between the observed peaks in both ionization modes correspond to a SO_3–PMG cleavage with an H substituting the SO_3–PMG pair (net loss of 353 mass units). Reprinted with permission from (Ohara et al. 2009)

method and make it basically comparable with other, previously developed ESI MS techniques. A similar approach based on the S/N ratio has already been successfully used for the quantitative analysis of HA oligomers obtained by digestion with hyaluronate lyase (Busse et al. 2006). Comparing the data of CS and HA, the last is more sensitively detectable i.e., the detection limit of HA is about 40 fmol (Busse et al. 2006), comparative to 5 pmol in the case of CS. Apart from the difference in the charge state of CS and HA, which determines their detectability by MS (Fuchs et al. 2008), both GAGs give rather similar MALDI data and can be determined by the same approach. It is expected that the developed assay can be easily implemented on MALDI MS devices of different configurations and is likely to be useful for many aspects of extracellular matrix research.

ESI MS

Conventional ESI MS technique involves the pumping of a solution into the ion source, which has been observed to produce relatively weak ion signals for native oligosaccharides compared to those for peptides and proteins. NanoESI produces carbohydrate ion signals that are comparable with peptides (Zaia 2004). Therefore, for the structural analysis of GAGs, nanoESI MS is an attractive technique due to the sensitivity and the wealth of structural information that can be obtained (Zaia and Costello 2001; Zaia 2004; Amon et al. 2008; Nielsen et al. 2008). The objectives of ESI MS in CS/DS oligosaccharide analysis are: (a) generation of high ionization yield; (b) detection of long and short chains in mixtures; (c) identification of sulfation degree; (d) determination of over-, regularly- and under-sulfated regions; (e) generation of diagnostic sequence ions in tandem MS experiments; (f) multistage MS of sulfated fragment ions for determination of sulfate group location along the chain and within the monomer ring. However, several technical problems of the ESI MS screening of CS/DS were reported as well. They are related to the difficulty to ionize long chains, hamper the in-source loss of labile SO_3 groups, and reduce the complexity of the obtained spectra in which the overlapping of isobaric peaks is frequently encountered. For ESI MS screening of complex biological mixtures containing nonsulfated and sulfated species, the in-source loss of SO_3 is one of the most severe drawbacks. Although employment of mild ESI source parameters substantially diminishes this fragmentation, sometimes loss of SO_3 cannot be completely eliminated. Source-induced fragmentation of CS/DS was studied very recently by Hu's group (Hu et al. 2009). It was noticed that at elevated cone voltages, above 50 V, polymeric chondroitin sulfate A molecules were completely dissociated. Further increase of the cone voltage led to (a) the observation of more prominent ions corresponding to shorter chains,

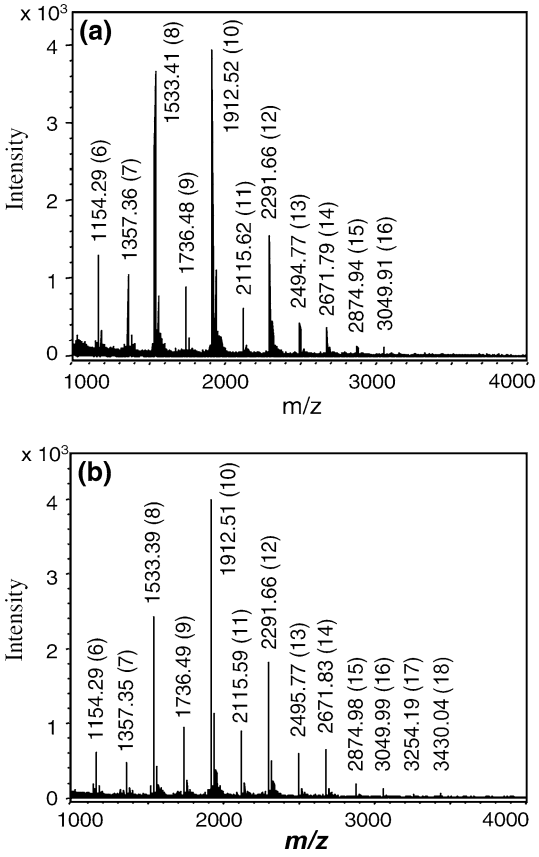

Fig. 5 MALDI TOF MS spectra of chondroitin synthesized by K4CP during the short-time reactions. The products synthesized by rK4CP by using nonradioisotopic substrates for 30 min (**a**) and 1 h (**b**) reactions are shown. The major peaks of the products of both reactions correspond to deca-, octa-, and dodecasaccharide ions, and the MS spectrum of the 1 h reaction product displayed slightly longer molecules than did that of the 30 min reaction product. The numbers on the ion peaks denote the *m/z* values and the chondroitin chain sizes (-mer, in *parentheses*). Reprinted with permission from (Sugiura et al. 2007)

(b) the increase in abundance of monosaccharide-related ions, and (c) occurrence of ring-cleavage ions. ESI mass spectra of CS C acquired at various cone voltages were similar to those of CS A suggesting that the position of the sulfate group on the disaccharide has little effect on the formation of ions via glycosidic bond cleavages. DS differs from CS A and C by the presence of L-iduronic acid in its structure. The *O*-sulfo group is mostly found on the C4 of GalNAc as for CS A. The in-source induced fragmentation of negatively charged DS was found comparable to those observed for CS A and C. Evidently, the replacement of glucuronic acid by iduronic acid is not a determinant factor affecting CS/DS source-induced fragmentation.

However, numerous difficulties encountered in the MS analysis of CS/DS (Amon et al. 2008) limit the benefits of this technique when applied to complex mixtures, if no separation is employed prior to MS. When the depolymerization is performed by lyases, complex mixtures containing intact chains of variable length and degree of sulfation are formed. In ESI MS, because of chain constitution, the monoisotopic peaks corresponding to charge states that equal half the number of the repeating units are observed at the same *m/z* value. This peak overlapping results in another specific challenge in ESI MS of CS/DS since it makes the mass spectra difficult to interpret and jeopardizes the isolation of the precursor ion for tandem MS, in particular when low-resolution instruments are used. Therefore, as we discuss in the next chapters, in the case of complex mixtures of differently sulfated CS/DS species, combination of nanoESI MS with separation techniques is a fundamental requirement for discriminating the real under- and non-sulfated species from the possible artifacts generated by the in-source SO_3 loss.

Fragmentation analysis by CID MS^n

By CID MS^n it is possible not only to produce CS/DS monosaccharide sequences, but also their ring cleavages, which are useful in obtaining the finest structural determinants, such as type of glycosidic linkages or even the position of particular ring substitutes. For assignment of CS/DS fragment ions in tandem mass spectra by either CID, electron detachment dissociation (EDD) or infrared multiphoton dissociation (IRMPD) the nomenclature introduced by Domon and Costello (1988) for linear oligo- and polysaccharides is most widely used. The general rules of this nomenclature are depicted in Fig. 7.

A challenge of MS-based CS/DS analysis is related to the mutually exclusive CID sequencing principles, which are required for reliable determination of sulfation site(s) i.e., cleavage of the glycosidic bond while keeping the SO_3 attached. Additionally, Zaia's group (Zaia et al. 2007) noticed that the interplay of uronic acids and sulfates determine the product ion patterns in CID experiments on CS. Thus, unsulfated chondroitin dissociates to form C-type ions almost exclusively, while CS produces abundant B- and Y-type ions from glycosidic bond cleavage with C- and Z-type of ions present only in low abundances. These observations were explained in terms of competing proton transfer reactions that occur during the collisional heating process. Another interesting aspect of CID MS/MS of CS is that product ion abundances reflect sulfation position at GalNAc residues (Zaia et al. 2001; McClellan et al. 2002) and epimerization of HexA residues (Zaia et al. 2004).

Based on these findings CID MS/MS was used (Miller et al. 2006) to determine positions of sulfation and epimerization by comparing abundances of the fragment ions formed from unknown DS oligosaccharides with those produced by CS/DS standards with known epimerization

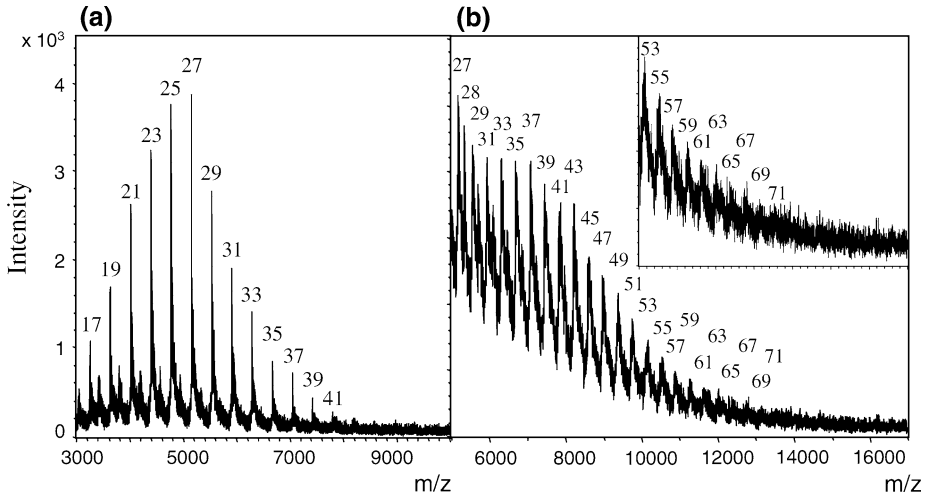

Fig. 6 MALDI TOF MS spectra of chondroitin oligo- and polysaccharides synthesized by rK4CP during the long-time reaction. **a** MALDI TOF MS corresponding to the peak fraction of chondroitin polymerization products separated on a Superdex Peptide HR10/30 column, *m/z* range: 3,000 to 10,000; **b** MALDI TOF MS corresponding to the higher fraction of chondroitin polymerization products separated on a Superdex Peptide HR10/30 column, *m/z* range: 5,000 to 17,000 and *m/z* range from 10,000 to 17,000 with intensity lengthened twofold (*inset* in panel b). The numbers on the ion peaks denote the chondroitin chain sizes (-mer). Reprinted with permission from (Sugiura et al. 2007)

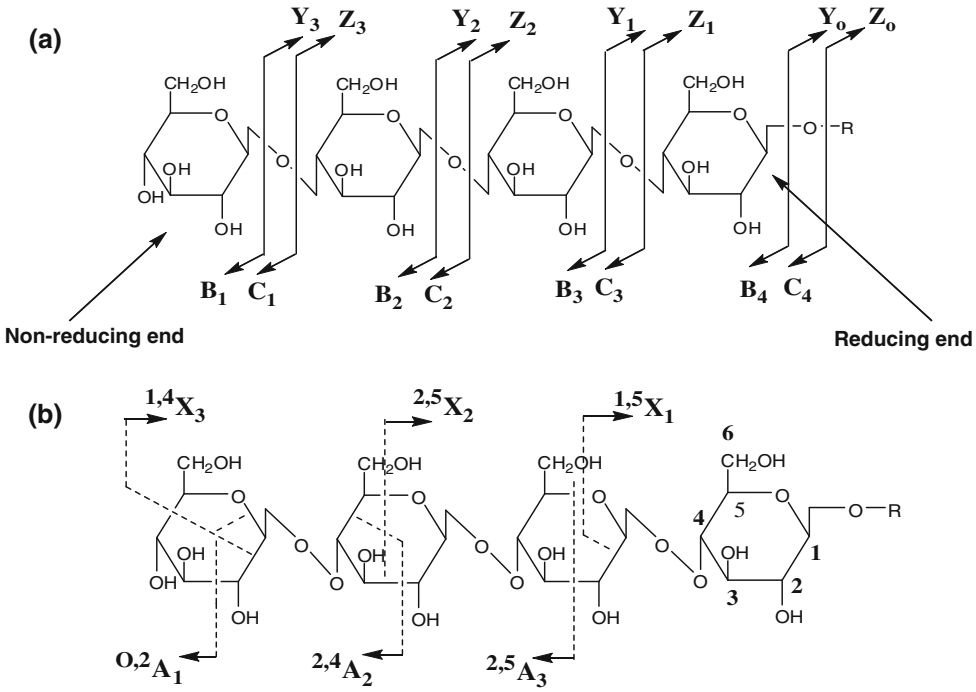

Fig. 7 Types of fragment ions in tandem mass spectra of linear polysaccharides and glycoconjugates and their assignment according to the nomenclature introduced by Domon and Costello (1988). **a** Ions produced by cleavage of glycosidic linkages; **b** ring-cleavage ions

and sulfate positions at GalNAc. In Fig. 8 tandem mass spectra of Δ4,5-unsaturated tetrasaccharides generated from CS A (a), CS B (b) and CS C (c) are presented. Although the three CS/DS isomers dissociate to form ions with identical *m/z* values, differences in abundances of the fragment ions are useful in discriminating them. Specifically, six signature ions (Table 1) the abundances of which differentiate the three isomers were found. In low-energy CID experiments, product ion abundances correlate with the lability of the cleaved covalent bonds. Thus, the sulfation and epimerization positions influence the lability of certain bonds in the oligosaccharide ions that are reflected by the observed ion abundances. Recently, in an application of this quantitative method based on CID MS/MS the percent composition of CS A-like (4GlcAβ1-3GalNAc4Sβ1-), CS B-like (4IdoAα1-3GalNAc4Sβ1-), CS C-like (4GlcAβ1-3GalNAc6Sβ1-) isomers for adult human cartilage and juvenile bovine cartilage, ligament, muscle,

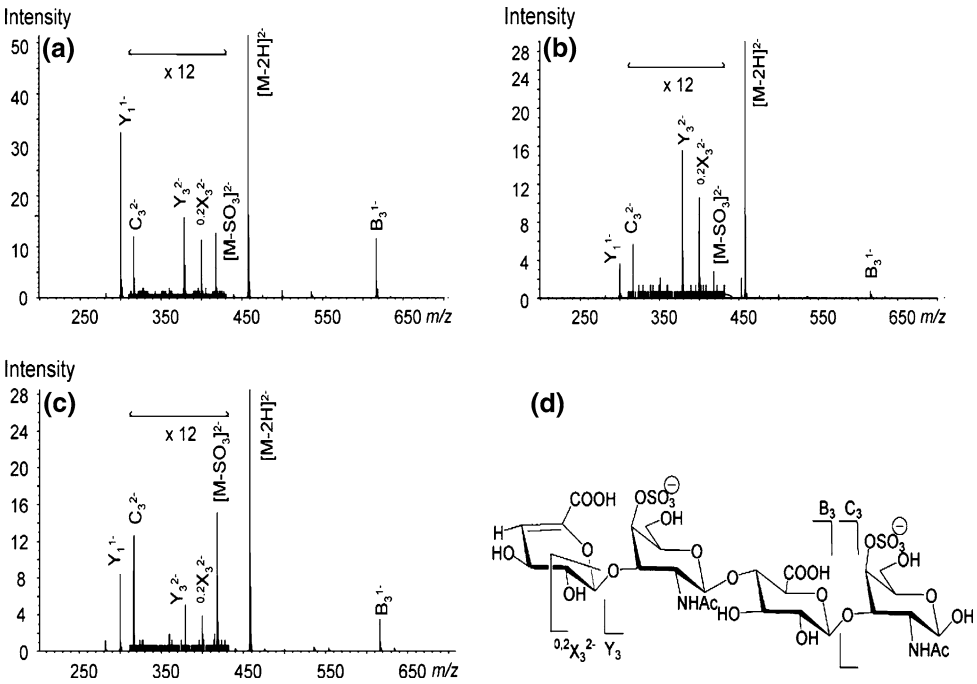

Fig. 8 Tandem mass spectra of Δ-unsaturated dp4 derived from CS A (**a**), CS B (**b**), and CS C (**c**). The structure of Δ-unsaturated dp4 from CS A is shown in **d** with product ion assignments. Solvent: 10% isopropanol with 0.1% NH_4OH; negative ion mode detection; ionization potential: –1,150 V; collision energies: –18 and –16 eV set to precursor ion remained as the most abundant. Reprinted with permission from (Miller et al. 2006)

Table 1 Percent total ion abundances for signature ions for Δdp4 derived from CS A, CS B, and CS C

Ion	CS A	CS B	CS C
Y_1^{1-}	33.91 ± 0.61	10.14 ± 0.56	19.88 ± 0.48
B_3^{1-}	11.22 ± 0.33	2.92 ± 0.73	7.74 ± 0.52
Y_3^{2-}	1.63 ± 0.27	3.18 ± 0.15	0.68 ± 0.05
$^{0,2}X_3^{2-}$	0.66 ± 0.05	2.41 ± 0.31	0.44 ± 0.04
C_3^{2-}	0.96 ± 0.03	0.78 ± 0.08	2.06 ± 0.18
$[M\text{-}SO_3]^{2-}$	0.89 ± 0.09	0.72 ± 0.64	2.23 ± 0.05

Reprinted with permission from (Miller et al. 2006)

tendon, and synovium samples was calculated (Hitchcock et al. 2008). CS A, CS B, and CS C standards were used to compare the relative amounts that were characteristic of each biological sample. Therefore, it is basically proven that this analytical platform can be used to identify CS and DS in human samples.

As inferable from these considerations, while multistage mass spectrometric investigation of regular and under-sulfated regions was performed successfully (Zaia et al. 2007; Miller et al. 2006; Estrella et al. 2007), so far the analysis of over-sulfated CS/DS domains by MS/MS (Zamfir et al. 2003, 2004; Mormann et al. 2007) resulted in rather reserved conclusions. Since sulfate esters are more labile than glycosidic linkages under most CID conditions, the unequivocal identification of excess sulfation sites has not been achieved in a single dissociation stage. We (Zamfir et al. 2009) introduced a novel and straightforward method to analyze atypical sulfation patterns in CS/DS chains derived from human fibroblast decorin (Dcn) using the strategy depicted in Fig. 9. ESI MS^n analysis encompasses: (a) determination of molecular ion masses (MS^1) giving their sizes and overall extents of sulfation followed by possible correlation of unusual sulfation content with HexA-epimerization and (b) identification of the positions of sulfate groups along the chain from the masses of the fragment ions generated by stepwise ion dissociation in multiple sequencing events (CID MS^2–MS^4).

To establish the location of sulfate groups within over-sulfated GlcA- and IdoA-rich domains, the triply charged ion at the GlcA-rich pentasulfated hexasaccharide [4,5-Δ-IdoAGalNAc-$(GlcAGalNAc)_2$](5S) detected by MS^1 has been chosen as the primary target for multi-stage MS analysis (Fig. 10). As previously demonstrated (Zamfir et al. 2003), by CID a high coverage of structurally informative sequence ions generated rather by glycosidic bond cleavage than SO_3 loss can be obtained if variable collision energy in the low eV range is employed. In the present case of successive CID in a single experiment, the fragmentation amplitude, its ramping interval, and time were adjusted in each step and for each re-sequenced fragment ion. Under such conditions, all spectra displayed a high proportion of over-sulfated fragment ions useful for localization of sulfate groups within the [4,5-Δ-IdoAGalNAc$(GlcAGalNAc)_2$](5S) hexasaccharides.

EDD MS^n

Electron detachment dissociation (EDD), performed on modern Fourier transform ion cyclotron resonance (FTICR) mass spectrometers, has been recently demonstrated as a

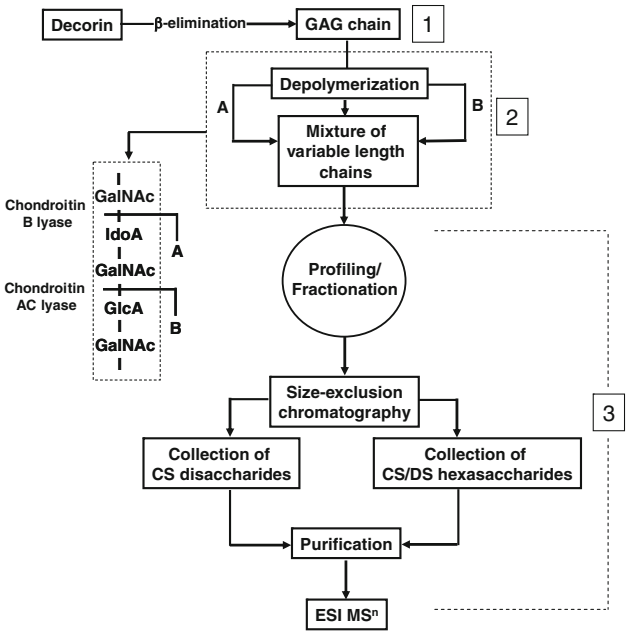

Fig. 9 Schematic of the strategy for GAG compositional and structural analysis based on the recognition specificity of chondroitin lyases and MS. *GAG* glycosaminoglycan, *GalNAc* *N*-acetylgalactosamine, *GlcA* D-glucuronate, *IdoA* L-iduronate. Reprinted and adapted with permission from (Zamfir et al. 2009)

powerful fragmentation technique for examination of glycan structural features (Wolff et al. 2007, 2008a; Leach et al. 2008; Chi et al. 2008). EDD produces a radical anion inducing a more extensive fragmentation than that obtained by activation of even electron ions using low energy or threshold dissociation methods. Unlike CID, the characteristics of glycan fragmentation by EDD, include abundant cross-ring fragmentation, cleavage of all glycosidic bonds, and the formation of even- and odd-electron product ions (Leach et al. 2008). Moreover, while CID or electron-induced dissociation methods of epimers produce identical fragmentation patterns, EDD generates spectra from which the epimers can be distinguished by their specific product ions. Therefore, EDD is the ideal MS tool for distinguishing glucuronic and iduronic acids (Wolff et al. 2008a).

Also, EDD produces more abundant glycosidic and cross-ring fragmentation for CS/DS oligosaccharides than it is observed by other dissociation methods, such as CID, collisionally activated dissociation (CAD), or IRMPD. Moreover, EDD exhibits a reduced loss of SO_3 from labile sites of sulfation compared to other methods of ion activation. This fragmentation behavior is a consequence of radical anion formation via electron detachment. EDD mechanism results in product ions that are distinctly different from the dissociation products of closed shell anions generated via low energy or threshold fragmentation methods, such as CAD or IRMPD. Analysis of the charge state and sodium cationization influence on the EDD fragmentation of a DS octasaccharide, followed by comparison with IRMPD was carried out by Wolff et al. (2008b). Similar to IRMPD, it was observed that the number of glycosidic bond and cross-ring cleavages produced by EDD decreased when the ionization of the CS/DS is increased by using sodium cations. Compared to IRMPD of the same precursor, EDD produces more glycosidic and cross-ring cleavages as well as less intense SO_3 loss (Fig. 11; Wolff et al. 2008c). Both features are of crucial importance for a reliable assignment of sulfate group position within the sugar ring.

Cross-ring fragmentation in EDD of regularly sulfated Δ4,5-IdoA-GalNAc(4S)-[IdoA-GalNAc(4S)]$_n$ hexa-, octa-, and decasaccharides was found to occur primarily within the IdoA residues rather than GalNAc (4S) residue. Moreover, unlike IRMPD, both A- and X-type of cleavages are produced. Overall, the large degree of fragmentation provided by EDD enhances the analysis of sulfated GAG oligosaccharides through a single MS/MS experiment.

From all the above considerations it is obvious that interpretation of CS/DS sequencing data represents a real challenge since a large number of variables must be considered. For this reason, major efforts into development of efficient bioinformatics tools to assist the interpretation of CS/DS mass spectra are being invested (Tissot et al. 2008).

Chip-ESI MS and MS^n

To improve the ESI process and increase the experiment throughput, sensitivity, and reproducibility, fully automated chip-based nanoESI MS was implemented for CS/DS analysis by us (Flangea et al. 2009a). In our study, a high capacity ion trap (HCT) instrument was interfaced with a NanoMate robot (Dethy et al. 2003; Kameoka et al. 2002) to create a system that combines the automatic chip-based ESI infusion with ultrafast screening and multistage fragmentation at superior sensitivity. The two instruments were coupled via an in-laboratory made mounting system, which allows robot O-xyz positioning with respect to the MS entrance. This system was optimized for CS/DS analysis in the negative ion mode, and its efficiency was initially tested for GalNAc (4S/6S) sulfation site discrimination in CS A and CS C unsaturated disaccharides. Fragmentation patterns obtained by chip-nanoESI CID MS^2 and MS^3 sequencing stages provided a number of fragment ions diagnostic for GalNAc monosulfation and for localization of sulfate group at either C6 or C4 position within GalNAc ring. The protocol developed here was extended, optimized, and applied to de novo identification of sulfation status and site(s) in isolated CS/DS disaccharide fractions extracted from wild-type mouse brain (Flangea et al. 2009b). MS screening revealed the presence of regularly- and non-sulfated DS species and over- and regularly sulfated CS species

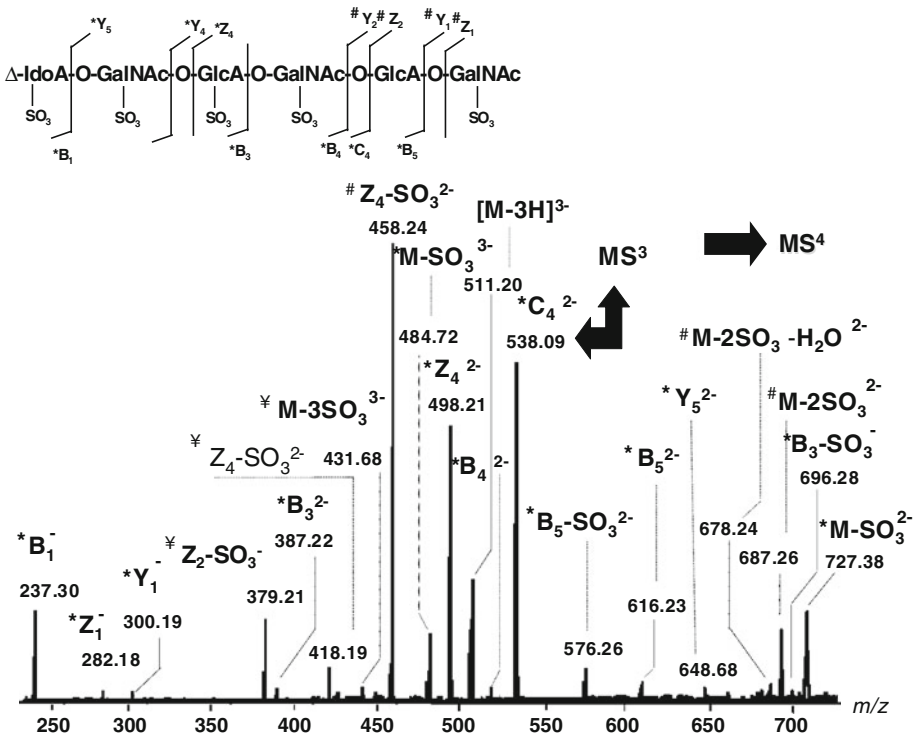

Fig. 10 Compositional and structural analysis of hexasaccharide fraction obtained from Dcn GAG chains after depolymerization with chon-B-lyase followed by gel filtration. MS^2 of the triply deprotonated ion at *m/z* 511.09. *Inset* proposed structure, its fragmentation pathways, and observed product ions. *Asterisks* denotes oversulfated, *hash symbol* denotes regularly sulfated, and *Yen sign* denotes undersulfated fragment ions. Negative ion mode detection. Solvent: MeOH; ESI MS parameters: Chip-ESI: 1.4 kV; capillary exit: −50 V. Back nitrogen pressure: 0.30 psi. Nitrogen nebulizer on MS at 50 psi. MS/MS by collision-induced dissociation (CID) using He as the collision gas. Fragmentation amplitude within 0.40–0.80 V. Reprinted and adapted with permission from (Zamfir et al. 2009)

(Fig. 12). Fragmentation analysis by CID MS^2–MS^3 of oversulfated 4,5-Δ-[GlcA-GalNAc] disaccharide bearing two SO_3^- groups disclosed an unusual sulfation pattern Δ4,5-[GlcA(3S)-GalNAc(6S)] (Fig. 13).

The first chip-based nanoESI MS screening indicated the major advantages provided by this modern ionization technique in GAG analysis: (a) a substantial increase in experiment sensitivity (picomole and subpicomole levels); (b) possibility to discover novel CS/DS species in complex mixtures due to elevated ionization efficiency and sensitivity; (c) a drastic reduction of in-source SO_3 loss as a consequence of the extremely mild electrospray ionization conditions required by chip-based technique; (d) superior run-to-run and in-run reproducibility as compared to capillary-based ESI; (e) long-lasting spray; (f) automated infusion, which makes the method amenable to high-throughput analysis.

Hyphenation of CE and LC to ESI MS for CS/DS mixture analysis

Mass spectrometry (MS) analysis of CS/DS components in complex mixtures was reported as challenging (Zaia and Costello 2001; Zaia 2004; Zamfir and Peter-Katalinić 2004; Amon et al. 2008) because of: (a) ion suppression; (b) isobaric peak overlapping; and (c) high spectrum complexity due to the formation of ions bearing different charge states and sometimes one or more alkali adducts, which generate signals of very different *m/z* values. For these reasons, screening of complex CS/DS mixtures and structural analysis of individual components by sequencing in MS/MS experiments required the combination of MS with efficient separation techniques, such as CE or LC.

CE/ESI MS and MS/MS

As previously emphasized by several reviews (Zamfir and Peter-Katalinić 2004; Volpi 2006; Seidler et al. 2007; Amon et al. 2008; Volpi et al. 2008; Zaia 2009) for CS/DS analysis, CE in combination with ESI MS exhibits high versatility, experimental sensitivity reported, separation efficiency according not only to the sugar chain length, but also to the degree of sulfation and the amount of structural data on single components present in mixtures of regularly-, under-, and over-sulfated chains of different size.

The most accessible approach for ESI MS characterization of CS/DS components separated by CE is the

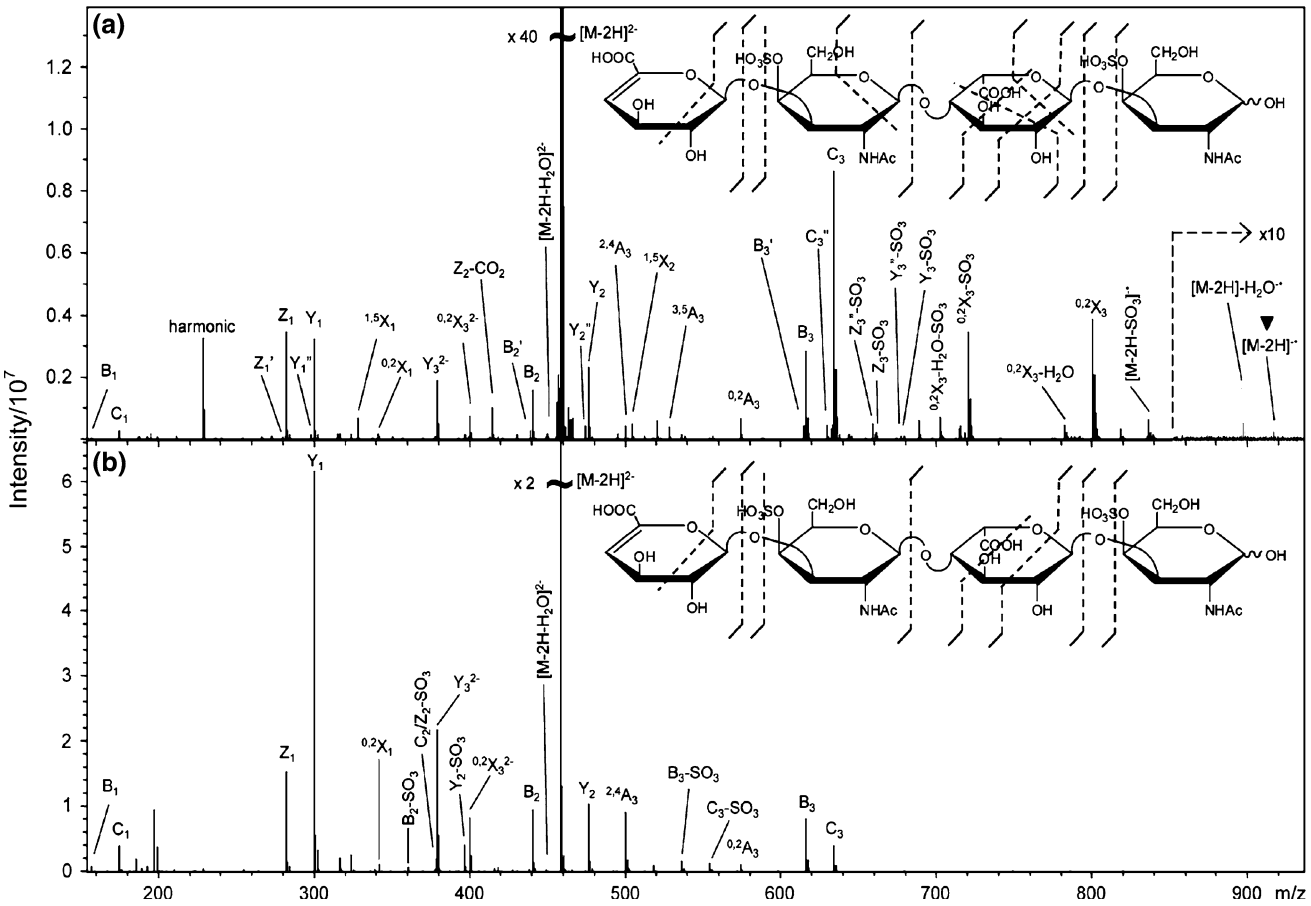

Fig. 11 MS/MS of $[M\text{-}2H]^{2-}$ precursor ion corresponding to DS tetrasaccharide digested with chondroitin ABC lyase. **a** EDD; **b** IRMPD. *Insets* product ions observed by the fragmentation methods (the ion assignment is according to the nomenclature of Domon and Costello illustrated in Fig. 7). The charge reduced species in the EDD mass spectrum is indicated with a *black down pointing triangle* over the peak label. Solvent: $MeOH:H_2O:NH_3$ (50:50:0.1); negative ion mode detection; electron irradiation cathode bias: −19 V; extraction lens: −17.5 ± 0.5 V; cathode heather: 1.6A. Reprinted with permission from (Wolff et al. 2008c)

off-line collection of fractions, which may be performed by either calculating the time window when a compound has migrated to the end of the capillary or using a prerun to obtain a CE profile and estimate the migration velocities. Unlike on-line coupling, off-line method provides higher flexibility toward system optimization since the CE and MS instruments can be adjusted independently and optimized separately. Additionally, post-separation treatments of the fraction, prior to MS analysis, like concentration by solvent evaporation, modification of buffer composition, dialysis, centrifugation, etc. are feasible. However, using the CE instrument as a fraction collector reduces the sample concentrations by the method principle itself; since the electrode and separation capillary need to be immersed in the buffer, fractions of a few nanoliters are collected into vials containing around 10 μL buffer. Lack of sensitivity is therefore the specific drawback of this approach often limiting the extension of its applicability toward minute amount of GAGs derived from biological matrices, even if post-collection sample concentration may be applied. In the analysis of GAG mixtures, off-line CE-MS is recommended only: (a) for simple mixtures or mixtures for which a partial separation of components is enough to reduce the ion suppression and enhance single component identification; (b) when flexibility toward system optimization is indispensable; (c) for cases where rather large amounts of analytes are available, and (d) as a prerequisite for on-line CE/ESI MS and first step in strategy development and system optimization.

For CS/DS, off-line collection of fractions was found suitable when performed using either a CE prerun with UV absorption or with laser-induced fluorescence (LIF) detection to determine the migration times and set the fraction collection interval. Collected fractions may be subsequently analyzed by ESI MS and tandem MS in order to identify the partially separated components in terms of chain length, epimerization, and sulfation pattern. However, from the separation point of view, a fundamental and general concern is that the best suited CE buffers are usually incompatible with CS/DS negative ion mode

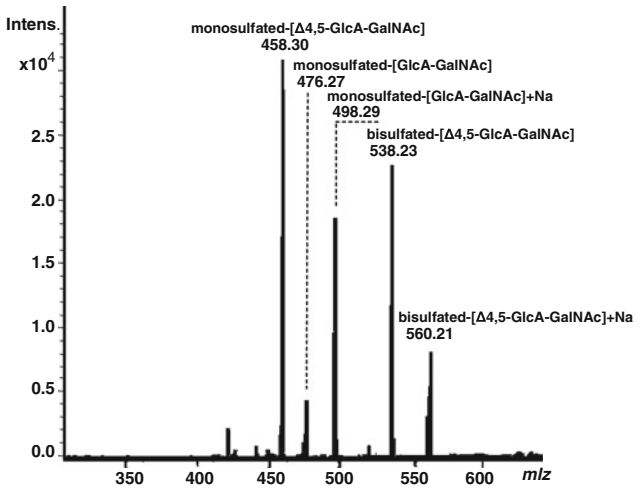

Fig. 12 Fully automated chip (–) nanoESI HCT MS of brain CS disaccharide obtained after depolymerization with chondroitin AC I lyase and separation on GFC-Superdex peptide column. Solvent: MeOH; ESI MS parameters: Chip-ESI: 1.4 kV; Cap Exit: 50 V. Back nitrogen pressure: 0.30 psi. Nitrogen nebulizer on MS at 50 psi. Reprinted with permission from (Flangea et al. 2009b)

electrospray process. Therefore, the compatibility of the CE background electrolyte (BGE) as spraying agent for CS/DS is one of the major difficulties encountered when interfacing either off-line or on-line the CE to ESI MS.

Normal polarity CE in off-line conjunction with (–) nanoESI hybrid quadrupole time-of-flight (QTOF) MS–MS/MS by CID was reported (Zamfir et al. 2002) for the analysis of CS/DS-derived oligosaccharides obtained from bovine aorta using 50 mM aqueous ammonium acetate/ammonia at pH 12.0 as BGE. CS/DS chain was released by β-elimination reaction and partially depolymerized using chondroitin B lyase. Resulting oligosaccharide mixture was dissolved in 10 μL BGE. For CE/UV screening, the sample was injected into CE capillary by applying a constant nitrogen pressure and separated at 25 kV direct polarity. According to the UV profile 10 different fractions were collected and submitted to nanoESI-QTOF MS screening using negative ion mode detection. Regularly sulfated hexa-, octa-, and decasaccharides, one undersulfated octasaccharide and one oversulfated hexasaccharide were identified. Several new aspects were revealed by this study: (a) CE/UV could provide signals of quite high intensity for 10 components, although the detection by UV absorption is not the most appropriate method for CS/DS profiling; (b) by CE, species with high molar sulfate content could be clearly separated from the non-sulfated ones, present in the CS/DS mixture; (c) CE separation was found ideal for strict determination of the degree of sulfation in single CS/DS species and for delineating the real under- and nonsulfated species from the possible artifacts induced by the in-source decay of the SO_3 groups in the MS; (d) besides enhancing MS detection of minor components, CE separation eliminated the widely known possibility of misinterpreting the CS/DS composition because of the overlapping of the isobaric peaks; (e) under optimized nanoESI MS conditions, the in-source desulfation of the molecules could be avoided and the formation of multiply charged ions was favored. This feature provided a significant contribution to the successful detection of regularly and oversulfated species in the CE fractions.

The last stage of this methodological development included the use of tandem mass spectrometry to provide the elucidation of monosaccharide building block sequences, information on the repeating GlcA-GalNAc, GlcA-GalNAc(S) units, as well as data on the glycosidic linkages. A fully sulfated octasaccharide detected in the first CE fraction and a sulfated disaccharide from the second CE fractions were the precursor ions in the MS/MS experiments. The most important outcome of the fragmentation process of both species was the clear indication of the sulfate group substitution pattern along the GAG chain.

An improved off-line CE-MS protocol in 3 stages was applied for the determination of biologically active sequence of CS/DS chains from decorin secreted by human skin fibroblasts, which is able to interact with fibroblast growth factor-2 (FGF-2) (Zamfir et al. 2003). The method was based also on CE fraction collection followed by detailed analysis using nanoESI-QTOF-MS and CID MS/MS in the negative ion mode. Decorin CS/DS chain was released by a β-elimination reaction; to discriminate between GlcA- or IdoA-rich domains the chain was partially digested with chondroitin B lyase and the products separated by gel-permeation chromatography. The fraction which eluted prior to hexasaccharides was used for CE and MS analysis in 50 mM ammonium acetate, pH 12.0, in water/MeOH 40:60 [v/v], a BGE which effectively met the requirements for CE separation and ESI process. The heterogeneity of this mixture, which contained CS/DS chains longer than hexamer was first assessed to a reasonable extent by CE with UV detection (Fig. 14). The 11 distinct components identified by CE/UV profiling were subsequently collected in 2 fractions for MS analysis. NanoESI-QTOF experiments indicated again that the species were separated by CE not only according to chain length, but also to sulfate content. Moreover, in analogy to the earlier reports (Desaire et al. 2001; Zaia and Costello 2001; Zaia et al. 2001) on ESI MS methods for GAG oligosaccharide analysis, it was observed that in the negative ESI MS, the in-source desulfation may be reduced by acquiring the spectra under mild values of the sampling cone potential. Using this protocol, it was possible to detect up to 12-mer oligosaccharides with different degrees of sulfation (Fig. 15; Table 2). Determination of SO_3 positions in a previously un-described 4,5-Δ-IdoAGalNAc[GlcAGalNAc]$_2$(5S)

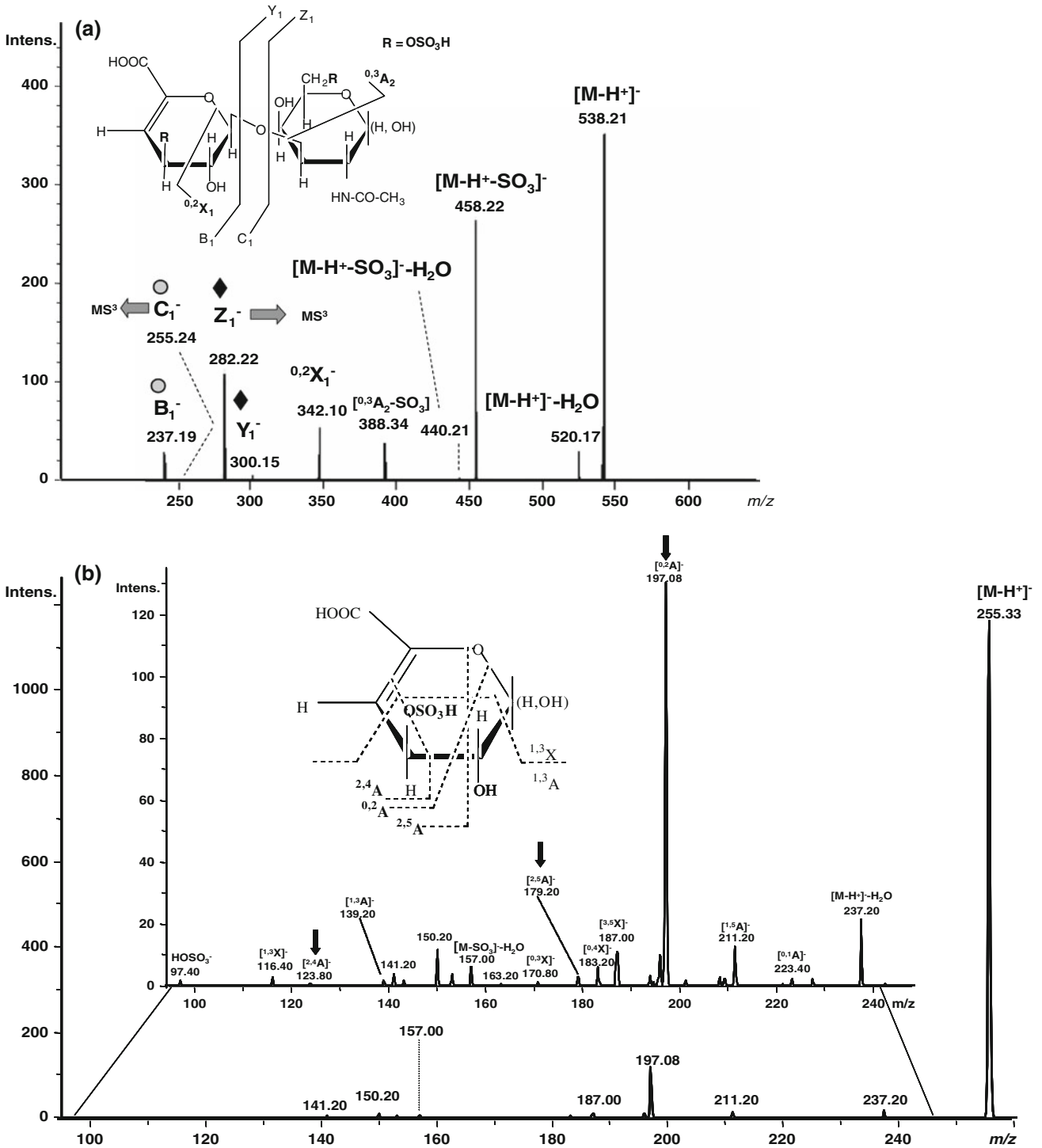

Fig. 13 Multiple stage chip (–) nanoESI CID MS structural analysis of bisulfated [4,5-Δ-GlcA-GalNAc]. **a** Fully automated chip (–) nanoESI HCT CID MS^2 of the singly deprotonated ions at *m/z* 538.21 assigned according to mass calculation to bisulfated 4,5-Δ-[GlcA-GalNAc]. Diagnostic ions for GalNAc monosulfation are marked by *filled diamonds*; diagnostic ions for GlcA monosulfation are marked by *filled circles*. *Inset* structure of bisulfated CS disaccharide. **b** Fully automated chip (–) nanoESI HCT CID MS^3 of the C_1^- fragment ion detected at *m/z* 255.24 in MS^2. *Inset* zoomed *m/z* (97–270) area and proposed ion structure. Diagnostic ions for GlcA (3S) is marked by *arrows*. Solvent: MeOH; ESI MS parameters: Chip-ESI: 1.4 kV; capillary exit: −50 V. Back nitrogen pressure: 0.30 psi. Nitrogen nebulizer on MS at 50 psi. MS/MS by collision-induced dissociation (CID) using He as collision gas. Fragmentation amplitude within 0.40–0.80 V. Reprinted and adapted with permission from (Flangea et al. 2009b)

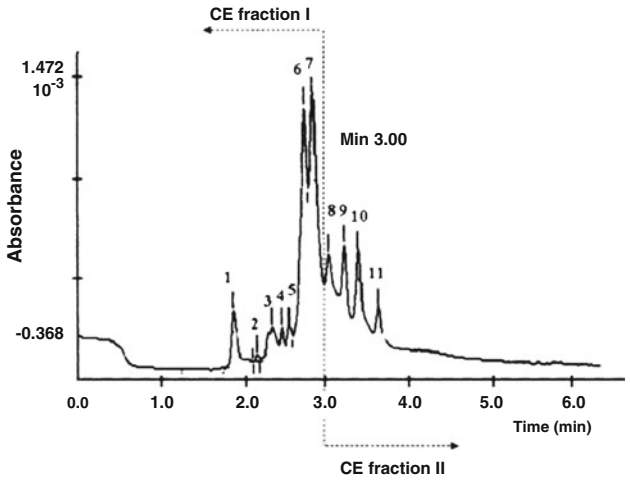

Fig. 14 CE/UV profile of CS/DS oligosaccharides from human decorin. BGE: ammonium acetate/ammonia, pH 12.0; CE separation voltage: 25 kV; 3 s injection by pressure; 12 nl injected volume; detection at 214 nm. Reprinted with permission from (Zamfir et al. 2003)

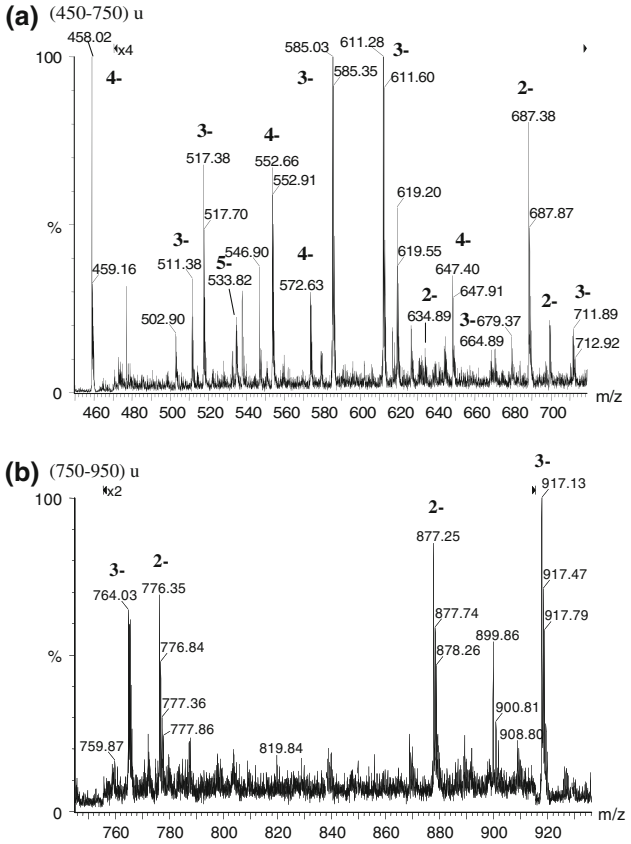

Fig. 15 Negative ion mode nanoESI-QTOF-MS of the CE fraction collected within the first 3 min after the application of the separation voltage. **a** *m/z* range (450–750); **b** *m/z* range (750–950). BGE: 50 mM ammonium acetate/ammonia; pH 12.0; CE separation voltage: 25 kV; 6 s injection by pressure; 20 nl injected volume; ESI voltage: 700 V; cone voltage: 15 V. Reprinted with permission from (Zamfir et al. 2003)

motif was achieved by a novel CID protocol at variable energy (VE) in which the collision energy was tuned during the ongoing experiment within 10–30 eV range. According to the generated MS/MS data, three sulfates were found distributed in the IdoAGalNAcGlcA moiety, offering two structural variants: (a) one containing sulfated IdoA, adjacent GalNAc disulfated and the two remote GalNAc moieties each monosulfated; and (b) one with IdoA, adjacent GlcA and all GalNAc residues monosulfated.

The low CS/DS yield produced after the application of specific sample extraction/purification protocols claimed for the development of on-line CE/nanoESI MS configurations able to address the issue of sensitivity. Since sheathless couplings provide the highest sensitivity, in a recent study (Zamfir et al. 2004), the CE column was butted to a commercial nanosprayer needle to shape a flexible interface suitable for separation and mass analysis of low CS/DS amounts. The resulting two-pieces-column was incorporated into a stainless steel clenching device to allow the application of the ESI voltage onto the needle and finally the whole interface was mounted directly on the ESI high voltage plate of a QTOF MS. The spray could be initiated at values of 600–900 V applied to the nanoESI needle and 12–30 V for the sampling cone potential without the need of nebulizer gas. This sheathless CE-MS method using direct CE polarity and negative ion mode ESI was applied to extended CS/DS GAG chains of recombinant expressed decorin from HEK293 cells (Zamfir et al. 2004) transfected with human decorin cDNA. GAG chain was released by β-elimination reaction and partially depolymerized with chondroitin B lyase. Resulting CS/DS mixture dissolved in 50 mM ammonium acetate/ammonia pH 12.0 as BGE was hydrodynamically injected, separated under 30 kV CE voltage and detected under 700 V nanoESI and 15 V cone potential. Mass spectra of separated components revealed that the species present in the mixture were well resolved by CE and efficiently ionized under the preset ESI conditions. Ions originating from oversulfated CS/DS species of up to 20-mer, not detectable by MS before, could be identified. It was also found that the migration behavior followed the ascending order of the molecular charge, originating from sulfate moieties, and was influenced by the presence of unsaturation located at the non-reducing end of the chain. The sensitivity obtained in these experiments reached considerably higher levels than those previously reported in off-line CE-MS studies; the system allowed detection of picomol amount of material, which is the level usually obtained after sample preparation protocols.

For structural elucidation, on-line CE/ESI MS/MS was performed by high-speed automated CID MS to MS/MS switching in data-dependent analysis mode, applied to an

Table 2 Assignment to CS/DS structures of the ions detected by negative ion mode nanoESI-QTOF-MS in the first CE fraction collected within the first 3 min after the application of the separation voltage

m/z	Type of ion	Proposed structure
458.02	$[M-4H]^{4-}$	IdoAGalNAc[GlcAGalNAc]$_3$ (4S)[a]
511.38	$[M-3H]^{3-}$	IdoAGalNAc[GlcAGalNAc]$_2$ (5S)[b]
517.38	$[M-3H]^{3-}$	IdoAGalNAc[GlcAGalNAc]$_2$ (5S)[b]
533.88	$[M-5H]^{5-}$	IdoAGalNAc[GlcAGalNAc]$_5$ (5S)
552.66	$[M-4H]^{4-}$	IdoAGalNAc[GlcAGalNAc]$_4$ (4S)
572.63	$[M-4H]^{4-}$	IdoAGalNAc[GlcAGalNAc]$_4$ (5S)[a]
585.03	$[M-3H]^{3-}$	IdoAGalNAc[GlcAGalNAc]$_3$ (3S)
611.28	$[M-3H]^{3-}$	IdoAGalNAc[GlcAGalNAc]$_3$ (4S)[a]
647.40	$[M-4H]^{4-}$	IdoAGalNAc[GlcAGalNAc]$_5$ (4S)
664.89	$[M-3H]^{3-}$	IdoAGalNAc[GlcAGalNAc]$_3$ (6S)[b]
687.38	$[M-2H]^{2-}$	IdoAGalNAc[GlcAGalNAc]$_2$ (3S)[a]
711.89	$[M-3H]^{3-}$	IdoAGalNAc[GlcAGalNAc]$_4$ (3S)[a]
764.03	$[M-3H]^{3-}$	IdoAGalNAc[GlcAGalNAc]$_4$ (5S)[a]
877.25	$[M-2H]^{2-}$	IdoAGalNAc[GlcAGalNAc]$_3$ (3S)
917.13	$[M-3H]^{3-}$	IdoAGalNAc[GlcAGalNAc]$_5$ (6S)[a]

Adapted with permission from (Zamfir et al. 2003)

nS denotes the number of sulfate groups in the molecule

[a] Regularly sulfated species

[b] Oversulfated species

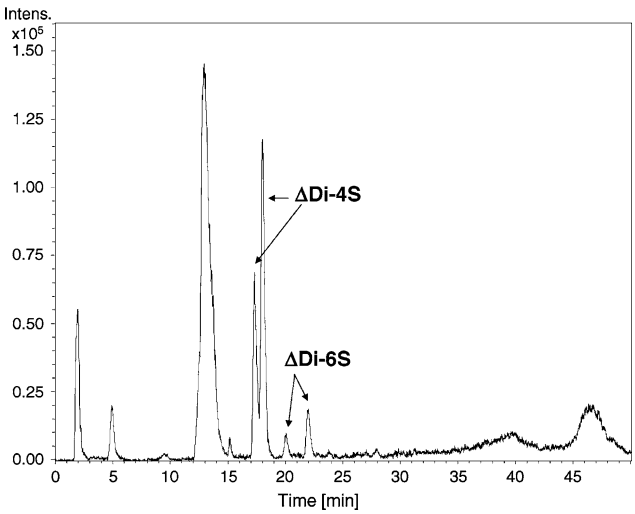

Fig. 16 LC/ESI MS profile of CS/DS disaccharides from human lung tissue. Eluent A: 0.1% formic acid in H_2O. Eluent B: 0.1% formic acid in ACN. Separation performed with 5–90% in 60 min gradient of B eluent. Detection: negative mode ESI. Acquisition: 50–1,200 amu MS scan range; 5,500 *m/z* per second scan rate. Reprinted with permission from (Barroso et al. 2005)

oversulfated eicosasaccharide species. Automatic fragmentation provided information on sulfation pattern, including the localization of the additional sulfate group along the chain.

LC/ESI MS and MS/MS

Due to their capability to separate CS/DS oligosaccharides according to fine structural differences (Volpi and Maccari 2009), LC/ESI MS methods complement CE-MS, which sometimes require laborious interfacing and system optimization procedures. As hydrophilic species, CS/DS in their native form are basically not retained by reversed-phase (RP) HPLC matrices. Therefore, LC of CS/DS is carried out either by (a) using porous graphitized carbon (PGC) columns or (b) in RP-HPLC as derivatized oligosaccharide species.

An efficient and highly sensitive LC MS method that combines PGC with ESI for CS/DS analysis was reported a few years ago by Barroso's group (2005). Chromatographic separation of only 5 ng of injected standard CS/DS disaccharides took place in a PGC column using 0.1% formic acid in ultrapure water as eluent A and 0.1% formic acid in acetonitrile (ACN) as eluent B. Separated analytes were detected by an Agilent SL ion-trap MS equipped with an ESI source operating in negative mode. Analysis of standard ΔDi-4S and independently of ΔDi-6S resulted in two chromatographic peaks for each type of disaccharides. LC MS profile indicated the presence of isomers that could be further characterized by CID MS/MS. Application of the protocol to CS/DS disaccharides from human lung tissue (Fig. 16) and bronchoalveolar lavage fluid obtained after total digestion with chondroitinase ABC demonstrated clearly that PGC MS method is able to disclose the presence of CS/DS isomers, separate, detect, and structurally characterize them.

Employing a similar PGC ESI MS system, more recently, Oguma's group (2007) quantified trace levels of DS disaccharides in human serum and plasma from healthy subjects and patients suffering from mucopolysaccharidoses (MPSs). In Oguma's protocol, underivatized unsaturated disaccharides resulting from digestion with chondriotinase B (*Flavobacterium heparinum* EC 4.2.2.) were separated on LC using as the mobile phase a gradient elution of ACN–10 mM ammonium bicarbonate buffer (pH 10). The initial composition of 0% ACN was kept for 0.9 min, linearly modified to 30% over 0.1 min, maintained at 30% for 6.0 min, modified to 0% over 0.1 min, and finally maintained at 0% for 1.9 min. The flow rate was 0.2 mL/min. DS components from healthy and MPS patients were determined by a turbo ionspray MS in multiple reaction monitoring mode. The mass spectrometer was operated in the negative ion detection mode with the turbo ionspray temperature optimized at 650°C. ΔDi-4S DS structures were identified both in healthy controls and in MPSs patients, however, at elevated levels in MPS I and

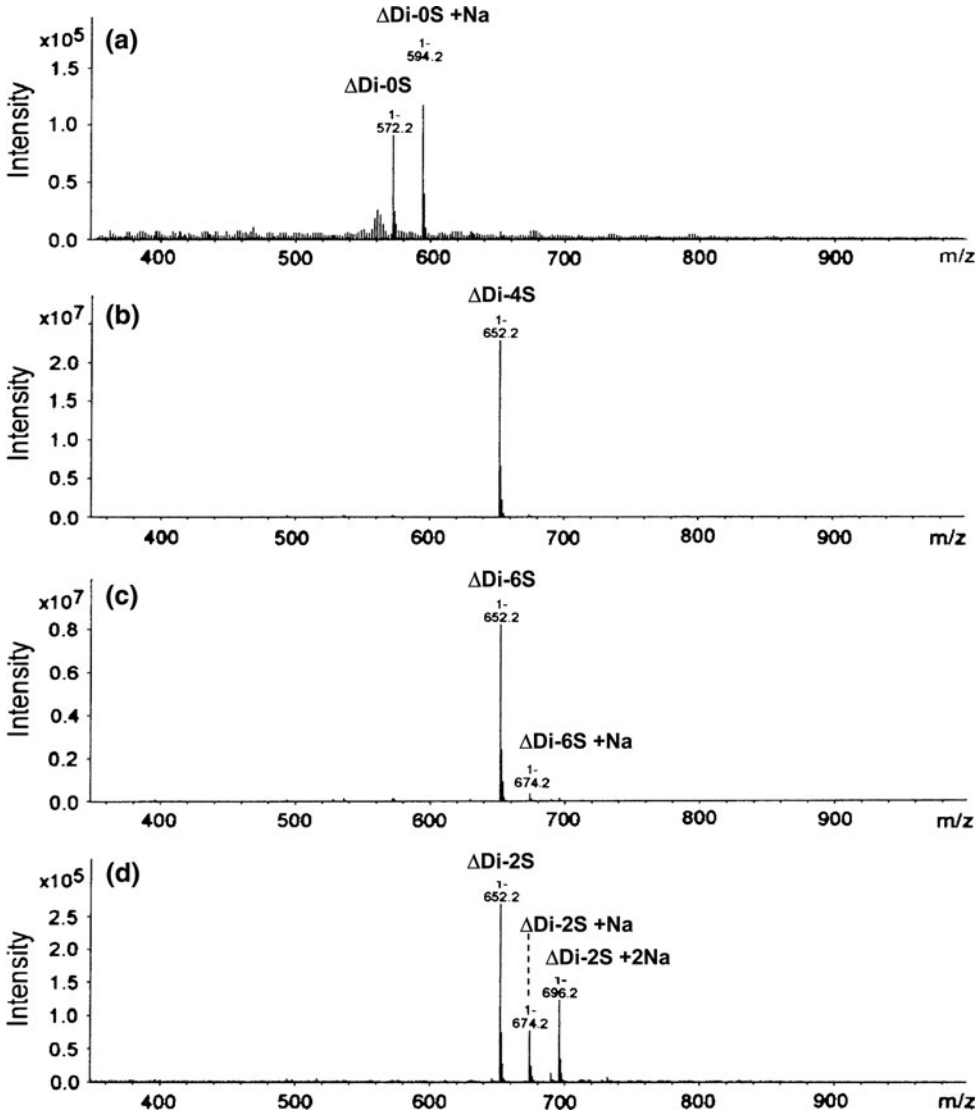

Fig. 17 Negative ion mode ESI MS of single unsaturated CS/DS disaccharides derivatized with AMAC and separated by RP–HPLC: **a** ΔDi-0S; **b** ΔDi-4S; **c** ΔDi-6S; **d** ΔDi-2S. Eluent A: 60 mM ammonium acetate (pH 5.6). Eluent B: ACN. Separation performed with 2–30% in 50 min gradient of B eluent. ESI voltage: 3,500 V. Acquisition: full scan mode, (100–2,000 Da, 10 full scans/s) with a maximum accumulation time of 300 ms. ΔDi-0S, ΔUA-(1 → 3)-GalNAc; ΔDi-4S, ΔUA-(1 → 3)-GalNAc-4S; ΔDi-6S, ΔUA-(1 → 3)-GalNAc-6S; ΔDi-2S, ΔUA-2S-(1 → 3)-GalNAc; UA-uronic acid. Adapted with permission from (Volpi 2010)

IV patients. Additionally, MS data indicated that GAGs stored in patient and control lysosomes show no difference in their sulfation levels (sulfo-groups/disaccharides). Used for comparative screening, healthy versus MPS patients, this methodology could be a useful tool in clinical diagnosis of lysosomal storage disease.

Reported results on LC MS analysis of CS/DS in their native form point out that the method exhibits a number of limitations among which, the most severe are related to the poor separation of monosulfated and disulfated isomeric species (Warda et al. 2008; Volpi 2010). Conversely, this drawback may be overcome by RP-HPLC MS applicable after appropriate sample derivatization. 2-Aminoacridone (AMAC), a fluorescent hydrophobic molecule, is one of the largely utilized derivatization agents for glycans, recently applied also to CS/DS for quantitative determinations by RP-HPLC (Ambrosius et al. 2008; Deakin and Lyon 2008). Recently, an original approach enabling on-line RP-HPLC with ESI MS detection for separation and structural characterization of derivatized CS/DS was conceived (Volpi 2010). In this protocol CS/DS disaccharides were derivatized at the reducing end with AMAC by reductive amination and subjected to RP-HPLC separation using 60 mM ammonium acetate (pH 5.6) as eluent A and ACN as eluent B with 2–30% in 50 min linear gradient. ESI MS detection of separated components was achieved on an ion-trap MS operating in negative ion mode, with the electrospray capillary voltage set at 3,500 V. As visible in the spectrum in Fig. 17, these working conditions provided not only an excellent separation of each CS/DS disaccharide species, but also high electrospray ionization efficiency of single components.

Besides the exhibited efficiency of separation and identification, LC MS is uniquely suited for accurate quantification of CS/DS glycoforms. Volpi's RP-HPLC MS protocol demonstrated also that the technique has the ability

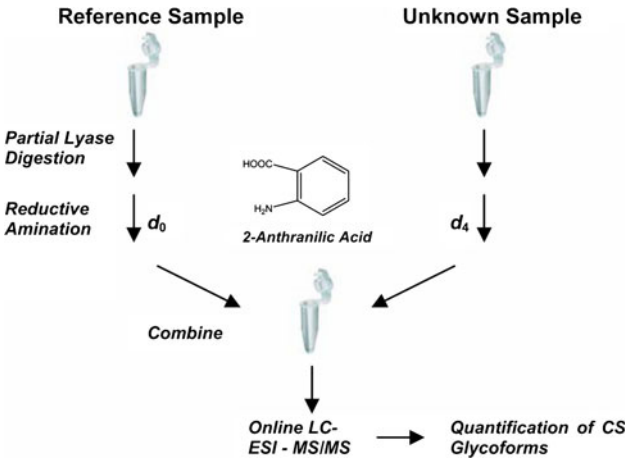

Fig. 18 Schematic of LC/ESI MS/MS platform for glycoform quantification of CS/DS mixtures using stable isotopic labeling. Reprinted with permission from (Hitchcock et al. 2006)

to perform an accurate quantitative analysis of disaccharide composition under elevated sensitivity (down to 1 μg injected sample). In another report on the development and application of LC MS as a tool for CS quantification, a stable isotopic labeling using either the light (d_0) or heavy (d_4) form of 2-anthranilic acid (2-AA) was proposed (Hitchcock et al. 2006). The incorporation of a stable isotopic tag allows usage of internal standard CS oligosaccharides. In this platform (Fig. 18) the unknown CS/DS chains were partially depolymerized using chondroitinase ABC, to generate a mixture of abundant (4–5)-unsaturated (Δ-) hexa-, tetra- and disaccharides. A reference CS was derivatized via reductive amination reaction with d_0-2AA and the unknown CS was derivatized with d_4-2AA. Reference (d_0) and unknown (d_4) CS samples were mixed, separated by LC, detected using on-line negative ion ESI MS and sequenced by CID MS/MS. This way, quantification of glycoforms within CS/DS samples could be made using relative ion abundances of specific diagnostic ions from MS/MS of separated components.

Conclusions and perspectives

To define and understand the structure-to-function interrelationship of CS/DS domains implicated in fundamental biological processes as well as to assess their role at the extracellular matrix level considerable efforts in development of high performance analytical methods have been invested. Current MS techniques characterized by sensitivity, resolution, and high accuracy offer a compelling platform on which such strategies for CS/DS structural analysis may be elaborated. As highlighted in this review, in the past 5 years, glycomics of CS/DS was dominated by ESI and MALDI MS. These methods were constantly optimized, improved, and applied alone or in conjunction with separation techniques not only for characterization of individual species, but also for compositional mapping and quantitative assays on heterogeneous mixtures resulted by partial depolymerization of long chains extracted from tissues and body fluids in very low amounts.

The elevated heterogeneity of structural motifs and atypical ionization/fragmentation conditions, which are more difficult to be fulfilled by high-throughput experiments, made this class of glycans less amenable to modern automated chip-based MS. Nevertheless, it was shown that adequate protocols may lead to successful implementation of chip technology also in CS/DS analysis, with superior results in terms of sensitivity, reproducibility, speed of analysis, and wealth of obtained structural information. Though in GAG analysis, chip-based ESI was so far established only for CS/DS disaccharides, the high performance of these systems will definitely drive them shortly toward applications on longer chains and more complex mixtures. It is at the same time expected that in the near future, the combination of chip-ESI with HPLC, CE, and powerful ion-trap/orbitrap, FTICR, and QTOF MS instruments will become of routine use also in GAG analysis.

Conflict of interest statement The authors declare that they have no conflict of interest.

References

Ambrosius M, Kleesiek K, Götting C (2008) Quantitative determination of the glycosaminoglycan Δ-disaccharide composition of serum, platelets, and granulocytes by reversed-phase high-performance liquid chromatography. J Chromatogr A 1201: 54–60

Amon S, Zamfir AD, Rizzi A (2008) Glycosylation analysis of glycoproteins and proteoglycans using capillary electrophoresis-mass spectrometry strategies. Electrophoresis 29:2485–2507

Bao X, Pavao MSG, dos Santos JC, Sugahara K (2005) A functional dermatan sulfate epitope containing iduronate(2-O-sulfate)alpha1–3GalNAc(6-O-sulfate) disaccharide in the mouse brain: demonstration using a novel monoclonal antibody raised against dermatan sulfate of ascidian *Ascidia nigra*. J Biol Chem 280:23184–23193

Barroso B, Didraga M, Bischoff R (2005) Analysis of proteoglycans derived sulphated disaccharides by liquid chromatography/mass spectrometry. J Chromatogr A 1080:43–48

Busse K, Averbeck M, Anderegg U, Arnold K, Simon JC, Schiller J (2006) The signal-to-noise ratio as a measure of HA oligomer concentration: a MALDI TOF MS study. Carbohydr Res 341:1065–1070

Chi L, Wolff JJ, Laremore TN, Restaino OF, Xie J, Schiraldi C, Toida T, Amster J, Linhardt RJ (2008) Structural analysis of bikunin glycosaminoglycan. J Am Chem Soc 130:2617–2625

Cointe D, Leroy Y, Chirat F (1998) Determination of the sialylation level and of the ratio α(2–3)/α(2–6) sialyl linkages of *n*-glycans by methylation and GC/MS analysis. Carbohydr Res 311:51–59

Deakin JA, Lyon M (2008) A simplified and sensitive fluorescent method for disaccharide analysis of both heparan sulfate and chondroitin/dermatan sulfates from biological samples. Glycobiology 18:483–491

Deepa SS, Kalayanamitra K, Ito Y, Kongtawelert P, Fukui P, Yamada S, Mikami T, Sugahara K (2007) Novel sulfated octa- and decasaccharides from squid cartilage chondroitin sulfate E: sequencing and application for determination of the epitope structure of the monoclonal antibody MO-225. Biochemistry 46:2453–2465

Desaire H, Sirich LT, Leary JA (2001) Evidence of block and randomly sequenced chondroitin polysaccharides: sequential enzymatic digestion and quantification using ion trap tandem mass spectrometry. Anal Chem 73:3513–3520

Dethy JM, Ackermann BL, Delatour C, Henion JD, Schultz GA (2003) Demonstration of direct bioanalysis of drugs in plasma using nanoelectrospray infusion from a silicon chip coupled with tandem mass spectrometry. Anal Chem 75:805–811

Domon B, Costello CE (1988) A systematic nomenclature for carbohydrate fragmentations in FAB-MS/MS spectra of glycoconjugates. Glycoconj J 5:397–409

Estrella RP, Whitelock JM, Packer NH, Karlsson NG (2007) Graphitized carbon LC-MS characterization of the chondroitin sulfate oligosaccharides of aggrecan. Anal Chem 79:3597–3606

Fedarko NS (2001) Purification of proteoglycans from mineralized tissues. Methods Mol Biol 171:19–25

Flangea C, Serb AF, Schiopu C, Tudor S, Sisu E, Seidler DG, Zamfir AD (2009a) Discrimination of GalNAc (4S/6S) sulfation sites in chondroitin sulfate disaccharides by chip-based nanoelectrospray multistage mass spectrometry. Cent Eur J Chem 7:752–759

Flangea C, Schiopu C, Sisu E, Serb A, Przybylski M, Seidler DG, Zamfir AD (2009b) Determination of sulfation pattern in brain glycosaminoglycans by chip-based electrospray ionization ion trap mass spectrometry. Anal Bioanal Chem 395:2489–2498

Fuchs B, Arnold K, Schiller J (2008) In: Meyers RA (ed) Encyclopedia of analytical chemistry. Wiley, Chichester, p 1

Hamai A, Hashimoto N, Mochizuki H, Kato F, Makiguchi Y, Horie K, Suzuki S (1997) Two distinct chondroitin sulfate ABC lyases: An endoeliminase yielding tetrasaccharides and an exoeliminase preferentially acting on oligosaccharides. J Biol Chem 272:9123–9130

Hernáiz MJ, Linhardt RJ (2001) Degradation of chondroitin sulfate and dermatan sulfate with chondroitin lyases. Methods Mol Biol 171:363–371

Hitchcock AM, Costello CE, Zaia J (2006) Glycoform quantification of chondroitin/dermatan sulfate using a liquid chromatography-tandem mass spectrometry platform. Biochemistry 45:2350–2361

Hitchcock AM, Yates KE, Costello CE, Zaia J (2008) Comparative glycomics of connective tissue glycosaminoglycans. Proteomics 8:1384–1397

Hu P, Fang L, Chess EK (2009) Source-induced fragmentation of heparin, heparan, and galactosaminoglycans and application. Anal Chem 81:2332–2343

Huang W, Boju L, Tkalec L, Su H, Yang HO, Gunay NS, Linhardt RJ, Kim YS, Matte A, Cygler M (2001) Active site of chondroitin AC lyase revealed by the structure of enzyme-oligosaccharide complexes and mutagenesis. Biochemistry 40:2359–2372

Kameoka J, Orth R, Ilic B, Czaplewski D, Wachs T, Craighead HG (2002) An electrospray ionization source for integration with microfluidics. Anal Chem 74:5897–5901

Kang P, Mechref Y, Klouckova I, Novotny MV (2005) Solid-phase permethylation of glycans for mass spectrometric analysis. Rapid Commun Mass Spectrom 19:3421–3428

Kang P, Mechref Y, Novotny MV (2008) High-throughput solid-phase permethylation of glycans prior to mass spectrometry. Rapid Commun Mass Spectrom 22:721–734

Khoo KH, Morris HR, McDowell RA, Dell A, Maccarana M, Lindahl U (1983) FABMS/derivatization strategies for the analysis of heparin derived oligosaccharides. Carbohydr Res 244:205–223

Kim YG, Kim SY, Hur YM, Joo HS, Chung J, Lee DS, Royle L, Rudd PM, Dwek RA, Harvey DJ, Kim BG (2006) The identification and characterization of xenoantigenic nonhuman carbohydrate sequences in membrane proteins from porcine kidney. Proteomics 6:1133–1142

Laremore TN, Linhardt RJ (2007) Improved matrix-assisted laser desorption/ionization mass spectrometric detection of glycosaminoglycan disaccharides as cesium salts. Rapid Commun Mass Spectrom 21:1315–1320

Laremore TN, Murugesan S, Park T-J, Avci FY, Zagorevski DV, Linhardt RJ (2006) Matrix-assisted laser desorption/ionization mass spectrometric analysis of uncomplexed highly sulfated oligosaccharides using ionic liquid matrices. Anal Chem 78:1774–1779

Laremore TN, Zhang F, Linhardt RJ (2007) Ionic Liquid Matrix for Direct UV-MALDI TOF-MS analysis of dermatan sulfate and chondroitin sulfate oligosaccharides. Anal Chem 79:1604–1610

Leach FE, Wolff JJ, Laremore TN, Linhardt RJ, Amster IJ (2008) Evaluation of the experimental parameters which control electron detachment dissociation, and their effect on the fragmentation efficiency of glycosaminoglycan carbohydrates. Int J Mass Spectrom 276:110–115

Lei M, Mechref Y, Novotny MV (2009) Structural analysis of sulfated glycans by sequential double-permethylation using methyl iodide and deuteromethyl iodide. J Am Soc Mass Spectrom 20:1660–1671

Lunin VV, Li Y, Linhardt RJ, Miyazono H, Kyogashima M, Kaneko T, Bell AW, Cygler M (2004) High-resolution crystal structure of *Arthrobacter aurescens* chondroitin AC lyase: an enzyme-substrate complex defines the catalytic mechanism. J Mol Biol 337:367–386

Matsui F, Oohira A (2006) Isolation, purification, and analysis of chondroitin sulfate proteoglycans. Adv Pharmacol 53:3–20

Matsuno Y, Yamada K, Tanabe A, Kinoshita M, Maruyama S-Z, Osaka Y-S, Masuko T, Kakehi K (2007) Development of an apparatus for rapid release of oligosaccharides at the glycosaminoglycan–protein linkage region in chondroitin sulfate-type proteoglycans. Anal Biochem 362:245–257

McClellan JE, Costello CE, O'Connor PB, Zaia J (2002) Influence of charge state on product ion mass spectra and the determination of 4S/6S sulfation sequence of chondroitin sulfate oligosaccharides. Anal Chem 74:3760–3771

Michel G, Pojasek K, Li Y, Sulea T, Linhardt RJ, Raman R, Prabhakar V, Sasisekharan R, Cygler M (2004) The structure of chondroitin B lyase complexed with glycosaminoglycan oligosaccharides unravels a calcium-dependent catalytic machinery. J Biol Chem 279:32882–32896

Miller MJC, Costello CE, Malmström A, Zaia J (2006) A tandem mass spectrometric approach to determination of chondroitin/dermatan sulfate oligosaccharide glycoforms. Glycobiology 16:502–513

Mormann M, Zamfir AD, Seidler DG, Kresse H, Peter-Katalinic J (2007) Analysis of over-sulfation in a chondroitin sulfate oligosaccharide fraction from bovine aorta by nanoelectrospray ionization quadrupole time-of-flight and Fourier transform ion cyclotron resonance mass spectrometry. J Am Soc Mass Spectrom 18:179–187

Naimy H, Leymarie N, Bowman MJ, Costello CE, Zaia J (2008) Amide-HILIC LC/MS for the characterization of Antithrombin III heparin binders. Biochemistry 47:3155–3161

Nielsen TC, Meikle PJ, Hopwood JJ, Fuller M (2008) Minimum substrate requirements of endoglycosidase activities toward

dermatan sulfate by electrospray ionization-tandem mass spectrometry. Glycobiology 18:1119–1128

Nimptsch A, Schibura S, Schnabelrauch M, Fuchs B, Huster D, Schiller J (2009) Characterization of the quantitative relationship between signal-to-noise (S/N) ratio and sample amount on-target by MALDI TOF MS: determination of chondroitin sulfate subsequent to enzymatic digestion. Anal Chim Acta 635:175–182

Oguma T, Tomatsu S, Montano AM, Okazaki O (2007) Analytical method for the determination of disaccharides derived from keratan, heparan, and dermatan sulfates in human serum and plasma by high-performance liquid chromatography/turbo ionspray ionization tandem mass spectrometry. Anal Biochem 368:79–86

Ohara K, Jacquinet JC, Jouanneau D, Helbert W, Smietana M, Vasseur JJ (2009) Matrix-assisted laser desorption/ionization mass spectrometric analysis of polysulfated-derived oligosaccharides using pyrenemethylguanidine. J Am Soc Mass Spectrom 20:131–137

Otsuki S, Nakajima M, Lotz M, Kinoshita M (2008) Hyaluronic acid and chondroitin sulfate content of osteoarthritic human knee cartilage: site-specific correlation with weight-bearing force based on femorotibial angle measurement. J Orthop Res 26:1194–1198

Pojasek K, Shriver Z, Kiley P, Venkataraman G, Sasisekharan R (2001) Recombinant expression, purification, and kinetic characterization of chondroitinase AC and chondroitinase B from *Flavobacterium heparinum*. Biochem Biophys Res Commun 286:343–351

Prabhakar V, Capila I, Bosques CJ, Pojasek K, Sasisekharan R (2005) Chondroitinase ABC I from *Proteus vulgaris*: cloning, recombinant expression and active site identification. Biochem J 386:103–112

Purushothaman A, Fukuda J, Mizumoto S, ten Dam GB, van Kuppevelt TH, Kitagawa H, Mikami T, Sugahara KJ (2007) Functions of chondroitin sulfate/dermatan sulfate chains in brain development. Critical roles of E and iE disaccharide units recognized by a single chain antibody GD3G7. J Biol Chem 282:19442–19452

Rye CS, Withers SG (2002) Elucidation of the mechanism of polysaccharide cleavage by chondroitin AC lyase from *Flavobacterium heparinum*. J Am Chem Soc 124:9756–9767

Schwartz NB, Domowicz M (2004) Proteoglycans in brain development. Glycoconj J 21:329–341

Seidler DG, Peter-Katalinić J, Zamfir AD (2007) Galactosaminoglycan function and oligosaccharide structure determination. Sci World J 19:233–241

Seyfried NT, Blundell CD, Day AJ, Almond A (2005) Preparation and application of biologically active fluorescent hyaluronan oligosaccharides. Glycobiology 15:303–312

Sugahara K, Yamada S (2000) Structure and function of oversulfated chondroitin sulfate variants: unique sulfation patterns and neuroregulatory activities. Trends Glycosci Glycotechnol 12:321–349

Sugiura N, Shimokata S, Watanabe H, Kimata K (2007) MS analysis of chondroitin polymerization: effects of Mn^{2+} ions on the stability of UDP-sugars and chondroitin synthesis. Anal Biochem 365:62–73

Taguchi T, Iwasaki M, Muto Y, Kitajima K, Inoue S, Khoo KH, Morris HR, Dell A, Inoue Y (1996) Occurrence and structural analysis of highly sulfated multiantennary *N*-linked glycan chains derived from a fertilization-associated carbohydrate-rich glycoprotein in unfertilized eggs of tribolodon hakonensis. Eur J Biochem 238:357–367

Tholey A, Heinzle E (2006) Ionic (liquid) matrices for matrix-assisted laser desorption/ionization mass spectrometry-applications and perspectives. Anal Bioanal Chem 386:24–37

Tissot B, Ceroni A, Powell AK, Morris HR, Yates EA, Turnbull JE, Gallagher JT, Dell A, Haslam SM (2008) Software tool for the structural determination of glycosaminoglycans by mass spectrometry. Anal Chem 80:9204–9212

Toole BP (2004) Hyaluronan: from extracellular glue to pericellular cue. Nat Rev Cancer 4:528–539

Tufvesson E, Malmstrom A (2002) Biglycan isoforms with differences in polysaccharide substitution and core protein in human lung fibroblasts. Eur J Biochem 269:3688–3696

Volpi N (2006) Advances in chondroitin sulfate analysis: application in physiological and pathological States of connective tissue and during pharmacological treatment of osteoarthritis. Curr Pharm Des 12:639–658

Volpi N (2007) Analytical aspects of pharmaceutical grade chondroitin sulfates. J Pharm Sci 96:3168–3180

Volpi N (2010) High-performance liquid chromatography and on-line mass spectrometry detection for the analysis of chondroitin sulfates/hyaluronan disaccharides derivatized with 2-aminoacridone. Anal Biochem 397:12–23

Volpi N, Maccari F (2009) Structural characterization and antithrombin activity of dermatan sulfate purified from marine clam *Scapharca inaequivalvis*. Glycobiology 19:356–367

Volpi N, Maccari F, Linhardt RJ (2008) Capillary electrophoresis of complex natural polysaccharides. Electrophoresis 29:3095–3106

Warda M, Zhang F, Radwan M, Zhang Z, Kim N, Kim YN, Linhardt RJ, Han J (2008) Is human placenta proteoglycan remodeling involved in pre-eclampsia? Glycoconj J 25:441–450

Wolff JJ, Chi L, Linhardt RJ, Amster IJ (2007) Electron detachment dissociation of glycosaminoglycan tetrasaccharides. J Am Soc Mass Spectrom 18:234–244

Wolff JJ, Laremore TN, Aslam H, Linhardt RJ, Amster IJ (2008a) Electron induced dissociation of glycosaminoglycan tetrasaccharides. J Am Soc Mass Spectrom 19:1449–1458

Wolff JJ, Laremore TN, Busch AM, Linhardt RJ, Amster IJ (2008b) Influence of charge state and sodium cationization on the electron detachment dissociation and infrared multiphoton dissociation of glycosaminoglycan oligosaccharides. J Am Soc Mass Spectrom 19:790–798

Wolff JJ, Laremore TN, Busch AM, Linhardt RJ, Amster IJ (2008c) Electron detachment dissociation of dermatan sulfate oligosaccharides. J Am Soc Mass Spectrom 19:294–304

Zaia J (2004) Mass spectrometry of oligosaccharides. Mass Spectrom Rev 23:161–227

Zaia J (2009) On-line separations combined with MS for analysis of glycosaminoglycans. Mass Spectrom Rev 28:254–272

Zaia J, Costello CE (2001) Compositional analysis of glycosaminoglycans by ESI MS. Anal Chem 73:233–239

Zaia J, McClellan JE, Costello CE (2001) Tandem mass spectrometric determination of the 4S/6S sulfation sequence in chondroitin sulfate oligosaccharides. Anal Chem 73:6030–6039

Zaia J, Miller MJC, Seymour JL, Costello CE (2007) The role of mobile protons in negative ion CID of oligosaccharides. J Am Soc Mass Spectrom 18:952–960

Zamfir AD, Peter-Katalinić J (2004) Capillary electrophoresis-mass spectrometry for glycoscreening in biomedical research. Electrophoresis 25:1949–1963

Zamfir AD, Seidler D, Kresse H, Peter-Katalinic J (2002) Structural characterization of chondroitin/dermatan sulfate oligosaccharides from bovine aorta by capillary electrophoresis and electrospray ionization quadrupole time-of-flight tandem mass spectrometry. Rapid Commun Mass Spectrom 16:2015–2024

Zamfir AD, Seidler D, Kresse H, Peter-Katalinic J (2003) Structural investigation of chondroitin/dermatan sulfate oligosaccharides from human skin fibroblast decorin. Glycobiology 11:733–742

Zamfir AD, Seidler D, Schonherr E, Kresse H, Peter-Katalinić J (2004) On-line sheathless capillary electrophoresis/nanoelectrospray ionization-tandem mass spectrometry for the analysis of glycosaminoglycan oligosaccharides. Electrophoresis 25:2010–2016

Zamfir AD, Flangea C, Sisu E, Serb AF, Dinca N, Bruckner P, Seidler DG (2009) Analysis of novel over- and under-sulfated glycosaminoglycan sequences by enzyme cleavage and multiple stage MS. Proteomics 9:3435–3444

Zhang Y, Kariya Y, Conrad AH, Tasheva ES, Conrad GW (2005) Analysis of keratan sulfate oligosaccharides by electrospray ionization tandem mass spectrometry. Anal Chem 77:902–910

Zhang H, Muramatsu T, Murase A, Yuasa S, Uchimura K, Kadomatsu K (2006) *N*-acetylglucosamine 6-*O*-sulfotransferase-1 is required for brain keratan sulfate biosynthesis and glial scar formation after brain injury. Glycobiology 16:702–710

Zhang Z, Park Y, Kemp MM, Zhao W, Im AR, Shaya D, Cygler M, Kim YS, Linhardt RJ (2009) Liquid chromatography-mass spectrometry to study chondroitin lyase action pattern. Anal Biochem 385:57–64

Zinellu A, Pisanu S, Zinellu E, Lepedda AJ, Cherchi GM, Sotgia S, Carru C, Deiana L, Formato M (2007) A novel LIF-CE method for the separation of hyaluronan- and chondroitin sulfate-derived disaccharides: Application to structural and quantitative analyses of human plasma low- and high-charged chondroitin sulfate isomers. Electrophoresis 28:2439–2447